PHYSICAL REVIEW D VOLUME 44, NUMBER 1 1 JULY 1991

Role of vector mesons in rare kaon decays

Pyungwon Ko
Enrico Fermi Institute and Department of Physics, University of Chicago, Chicago, Illinois 60637
(Received 28 November 1990)

We study the role of vector mesons in $K\to\pi\pi$, $K\to\pi l^+l^-$, $K_L\to\gamma l^+l^-$, and $K_L\to\pi^0\gamma\gamma$ using the chiral Lagrangian in the hidden-symmetry scheme with the Wess-Zumino anomaly. Two main features of our approach are (i) the slight modification of the effective weak chiral Lagrangian and (ii) the existence of the anomalous left-handed current constructed from the Wess-Zumino anomaly and intrinsic parity-violating interactions involving vector mesons. We predict that the decay mode $K_L\to\pi^0e^+e^-$ is dominated by the indirect *CP*-violating one-photon-exchange process, which occurs at the level of a few parts in 10^{10} in the branching ratio. We can also understand the recent data on $K_L\to\gamma e^+e^-$ and $K_L\to\pi^0\gamma\gamma$ in our framework, except for the branching ratio of $K_L\to\pi^0\gamma\gamma$.

I. INTRODUCTION

The role of vector mesons in $K_L\to\pi^0\gamma\gamma$ and $K_L\to\pi^0e^+e^-$ has been a controversial subject [1,2]. Chiral perturbation theory [1] and the pion rescattering model [3] predict that the pion loop gives a dominant contribution to $K_L\to\pi^0\gamma\gamma$ with a branching ratio around 7×10^{-7}, and the two-photon spectrum has a peak near $m_{\gamma\gamma}\simeq300$ MeV in both models. Also, the low-energy photon pair is almost negligible. On the other hand, there can be a large enhancement in the low-$m_{\gamma\gamma}$ region [4,5], if vector mesons come into play in this decay mode and one uses the naive nonet symmetry in $K_2\to P$ (with $P=\pi^0,\eta_8,\eta_0$). In this case, the branching ratio is $(1-3)\times10^{-6}$.

The recent measurement [6] of $K_L\to\pi^0\gamma\gamma$ from CERN is rather puzzling. The two-photon spectrum seems consistent with the predictions of the chiral perturbation theory (ChPT) and the pion rescattering model. However, the branching ratio for $m_{\gamma\gamma}\geq280$ MeV is larger than those predictions by a factor of 3–4. In this rather confusing situation, it would be nice to have a systematic calculation for $K_L\to\pi^0\gamma\gamma$ as well as for other processes where vector-meson contributions can be potentially important.

In this paper, we give self-consistent calculations for $K\to\pi\pi$, $K\to\pi l^+l^-$, $K_L\to\gamma\gamma$, $K_L\to\gamma l^+l^-$, and $K_L\to\pi^0\gamma\gamma$ in the hidden-symmetry scheme [7] in conjunction with the nonleptonic Hamiltonian used by Sakurai, Cronin and other groups [8]. In Sec. II, we give a brief review of the hidden-symmetry scheme with the Wess-Zumino anomaly. In our approach, the usual $O(p^4)$ and $O(p^6)$ terms arise from vector-meson exchange between the chiral mesons, and from the Wess-Zumino anomaly term including vector mesons. From the work of Ref. [5], it is known that the $O(p^6)$ terms through ρ^0 and ω exchange in $\gamma\gamma\to\pi^0\pi^0$ unitarize the chiral loop amplitude in an effective way up to $m_{\gamma\gamma}\sim1$ GeV, and controls the high-energy behavior of the chiral amplitudes. Once we make this assumption, things get much simplified and we anticipate we do not lose any important physics information. The major advantage of our model lies in the number of unknown parameters to be determined by the experimental data. In fact, we do not have any unknown parameters at the level of strong and electromagnetic interactions other than the meson masses and their decay constants, *once* we adopt the notion of vector-meson dominance in the normal sector ($a=2$ in the notation of Bando *et al.*; see Sec. II.) In Sec. III, we first discuss the structure of the left-handed currents. We find that there exist anomalous left-handed currents arising from the Wess-Zumino anomaly and the intrinsic parity-violating interactions involving vector mesons, and they give important contributions to $K_L\to\gamma l^+l^-$ and $K_L\to\pi^0\gamma\gamma$ through generating *weak* $V\pi\gamma$ vertices. The nonleptonic weak decays of kaons is described by the effective weak Lagrangian of current-current interactions. We make connections with the calculations in terms of quark fields with QCD corrections [9,10], and find that there is an additional term in the effective weak Lagrangian, which is proportional to $\mathrm{Tr}(j_{\mu L})$ where the trace is taken over the $U(3)_f$ or $SU(3)_f$ indices. This additional term cannot be thrown away as usually done in the case of $SU(3)_L\times SU(3)_R$, since the anomalous left-handed currents we consider in this paper have a nonvanishing trace even in that case. The coefficient of this new term measures the contributions of penguin operators of current-current types to the nonleptonic kaon decays. At this stage, we will have four parameters $C_8^{(1/2)}$, $C_{27}^{(1/2)}$, $C_{27}^{(3/2)}$ and δ_p with one constraint $C_{27}^{(3/2)}=5C_{27}^{(1/2)}$. C's characterize the strengths of the $(8_L,1_R)_{\Delta I=1/2}$, $(27_L,1_R)_{\Delta I=1/2}$, and $(27_L,1_R)_{\Delta I=3/2}$ pieces of the weak Hamiltonian, respectively. Deviation of δ_p from 1 measures the contributions of penguin operators. We fix C's from $K\to\pi\pi$. δ_p contributes to $K_L\to\pi^0\gamma\gamma$ in the $SU(3)_L\times SU(3)_R$ case, and both to $K_L\to\pi^0\gamma\gamma$ and to $K_L\to\gamma l^+l^-$ in the $U(3)_L\times U(3)_R$ case. In the following, we assume nonet symmetry in the vector-meson sector. Before studying the effects of δ_p on $K_L\to\gamma l^+l^-$ and

$K_L \to \pi^0\gamma\gamma$, we analyze $K \to \pi l^+ l^-$ in Sec. IV using the suitable value of δ_p. For the decay mode $K \to \pi l^+ l^-$, we need two more operators, $Q_{7V} \equiv (\bar{s}d)_{V-A}(\bar{l}l)_V$ and $Q_{7A} \equiv (\bar{s}d)_{V-A}(\bar{l}l)_A$, arising from the electromagnetic penguin diagram [11], the Z^0 penguin diagram, and the box diagram with two internal W's [12]. The real part of the Wilson coefficients of these operators cannot be calculated reliably. Therefore, we introduce another parameter C_7 as the coefficient of the new operator Q_{7V}, ignoring the operator Q_{7A}. We fix C_7 from the best fit to the decay mode $K^+ \to \pi^+ e^+ e^-$. There is a twofold ambiguity in C_7, and we can predict for $K^+ \to \pi^+ \mu^+ \mu^-$, $K_S \to \pi^0 e^+ e^-$, and $K_S \to \pi^0 \mu^+ \mu^-$. Our model predicts the decay rate for the $K_S \to \pi^0 e^+ e^-$ process to be comparable to the decay rate for $K^+ \to \pi^+ e^+ e^-$. The $K_S \to \pi^0 e^+ e^-$ process contributes to the indirectly *CP*-violating $K_L \to \pi^0 e^+ e^-$ process through the mixing between K_L and K_S. We predict that the branching ratio of the indirectly *CP*-violating $K_L \to \pi^0 e^+ e^-$ process is about 1.4 or 2.7×10^{-10}, which is substantially larger than other previous calculations. Another process in which vector mesons are important is $K_L \to \gamma e^+ e^-$. This has been recently remeasured and the form factor shows a clear deviation from the ρ form factor [13, 14]. In Sec. V, we give a comprehensive analysis of $K_L \to \gamma\gamma$ and $K_L \to \gamma l^+ l^-$. In $K_L \to \gamma l^+ l^-$, we have both *weak VV* and *weak* $V\pi\gamma$ vertices, the latter of which was not considered in the earlier analysis. In this section, we introduce one more parameter δ_n characterizing the possible deviation of $a(K_2\eta_0)$ from its naive value obtained from the effective weak Lagrangian. This takes care of the fact that the $U(1)_A$ symmetry is broken through the QCD axial anomaly. (We assume nonet symmetry elsewhere.) The recent data on $K_L \to \gamma e^+ e^-$, when combined with the branching ratio of $K_L \to \gamma\gamma$, provide us with important information on $\zeta \equiv a(K_2\eta)/a(K_2\pi^0)$, $\zeta' \equiv a(K_2\eta')/a(K_2\pi^0)$ and δ_p, or equivalently, on δ_n and δ_p. We will have two solutions for δ_n, each of which corresponds to π^- and η dominance in $K_L \to \gamma\gamma$, respectively. Then, δ_p is constrained to some region for each δ_n. Section VI is devoted to the study of $K_L \to \pi^0\gamma\gamma$ and its implication for the *CP*-conserving part of $K_L \to \pi^0 e^+ e^-$. In our calculations of $K_L \to \pi^0\gamma\gamma$, we find there is direct emission of vector mesons from weak vertices, which was not considered in a systematic way before. It turns out that the two-photon spectrum of $K_L \to \pi^0\gamma\gamma$ at low $m_{\gamma\gamma}$ shows sensitive dependence on δ_p. For δ_n corresponding to π dominance in $K_L \to \gamma\gamma$, the predicted two-photon spectrum does not agree with experiment. Therefore, we choose δ_n corresponding to η dominance in $K_L \to \gamma\gamma$, for which the low-energy photon pair is indeed suppressed as recently observed, and $B(K_L \to \pi^0\gamma\gamma) \simeq 5.7 \times 10^{-7}$ for $\delta_p = 0$. This will imply that the *CP*-conserving two-photon-exchange contribution to $K_L \to \pi^0 e^+ e^-$ is negligible compared to the *CP*-violating contribution. In Sec. VII, we summarize our results as a whole. Possible modifications and/or improvements of our model will be proposed. Comparisons with other approaches are briefly discussed in each section.

II. CHIRAL LAGRANGIAN IN THE HIDDEN-SYMMETRY SCHEME

A. Vector mesons in the hidden-symmetry scheme

The hidden-symmetry approach [7] exploits the fact that the nonlinear chiral Lagrangian describing the Nambu-Goldstone (NG) bosons for a $(G/H)_{\text{global}}$ coset space is equivalent to the linear σ model with symmetry group $G_{\text{global}} \times H_{\text{local}}$ [15]. Vector mesons are introduced as gauge bosons associated with the hidden local symmetry group H. Specifically, we consider the groups $G = U(3)_L \times U(3)_R$ and $H = U(3)_V$. The scalar and the pseudoscalar nonets are represented by 3×3 matrix fields $\xi_L(x)$ and $\xi_R(x)$, and the vector-meson nonet by $V_\mu(x)$. Under $[U(3)_L \times U(3)_R]_{\text{global}} \times [U(3)_V]_{\text{local}}$, they transform as

$$\xi_L(x) \to e^{iv(x)} \xi_L(x) e^{-i\epsilon_L} ,$$

$$\xi_R(x) \to e^{iv(x)} \xi_R(x) e^{-i\epsilon_R} ,$$

$$gV_\mu(x) \to ie^{iv(x)} [\partial_\mu - igV_\mu(x)] e^{-iv(x)} ,$$

where $v(x) = \sum_0^8 v^a(x) T^a$ is a 3×3 matrix field, and is the group parameter of the hidden symmetry group $[U(3)_V]_{\text{local}}$. The U(3) generators T^a's are normalized as $\text{Tr}(T^a T^b) = \frac{1}{2}\delta^{ab}$. g is the gauge coupling constant associated with $[U(3)_V]_{\text{local}}$. ϵ_L and ϵ_R are the group parameters of $[U(3)_L \times U(3)_R]_{\text{global}}$. To couple the NG bosons to external gauge fields such as γ, $W^\pm$, and Z, we gauge the full global symmetry group G by introducing the gauge fields, l_μ and r_μ, and the covariant derivative

$$D_\mu \xi_L = (\partial_\mu - igV_\mu)\xi_L + i\xi_L l_\mu ,$$

$$D_\mu \xi_R = (\partial_\mu - igV_\mu)\xi_R + i\xi_R r_\mu ,$$

which transform as $\xi_L(x)$ and $\xi_R(x)$, if the gauge fields transform appropriately:

$$\delta l_\mu(x) = \partial_\mu \epsilon_L(x) + i[\epsilon_L(x), l_\mu(x)] ,$$

$$\delta r_\mu(x) = \partial_\mu \epsilon_R(x) + i[\epsilon_R(x), r_\mu(x)] .$$

Here, $\epsilon_L(x)$ and $\epsilon_R(x)$ are the 3×3 matrix field group parameters of $[U(3)_L \times U(3)_R]_{\text{global}}$. If we want to introduce $SU(2)_L \times U(1)_Y$ electroweak gauge fields, we can set

$$r_\mu = eQ(A_\mu - \tan\theta_W Z_\mu) ,$$

$$l_\mu = r_\mu + \frac{e}{\sin\theta_W \cos\theta_W} T_Z Z_\mu + \frac{e}{\sqrt{2}\sin\theta_W} W_\mu ,$$

where $Q = \text{diag}(\frac{2}{3}, -\frac{1}{3}, -\frac{1}{3})$ is the 3×3 electric charge matrix of three light quarks, $T_z = \text{diag}(\frac{1}{2}, -\frac{1}{2}, -\frac{1}{2})$ is the coupling between the left-handed current and the Z^0 boson, and

$$W_\mu = \begin{pmatrix} 0 & W_\mu^+ \cos\theta_C & W_\mu^+ \sin\theta_C \\ W_\mu^- \cos\theta_C & 0 & 0 \\ W_\mu^- \sin\theta_C & 0 & 0 \end{pmatrix} .$$

θ_W and θ_C are the Weinberg angle and the Cabibbo angle, respectively. Since we are interested in $\Delta S=1$ weak decays of kaons, we set $Z_\mu=0$.

The various low-energy theorems concerning the processes involving the NG bosons can be derived in an effective way from the following Lagrangian [16] $\mathcal{L}_{\rm tot}$:

$$\mathcal{L}_{\rm tot}=\mathcal{L}_A+\mathcal{L}_B+\mathcal{L}_{\rm kin}(V)+\Gamma^{\rm anom}(\xi_L,\xi_R,V,l,r)\ ; \quad (1)$$

$$\mathcal{L}_A=-\frac{f_\pi^2}{4}\mathrm{Tr}[(D_\mu\xi_L)\xi_L^\dagger-(D_\mu\xi_R)\xi_R^\dagger]^2\ ,$$

$$\mathcal{L}_B=-a\frac{f_\pi^2}{4}\mathrm{Tr}[(D_\mu\xi_L)\xi_L^\dagger+(D_\mu\xi_R)\xi_R^\dagger]^2\ ,$$

$$\mathcal{L}_{\rm kin}(V)=-\tfrac{1}{2}\mathrm{Tr}(F_{\mu\nu}F^{\mu\nu})\ , \quad (2)$$

$$F_{\mu\nu}\equiv\partial_\mu V_\nu-\partial_\nu V_\mu-ig[V_\mu,V_\nu]\ ,$$

Here, $f_\pi=93$ MeV is the pion decay constant. We consider only the $O(p^2)$ term in the spirit of the low-energy theorems. If we take the unitary gauge in which $\xi_L^\dagger(x)=\xi_R(x)=\exp[i\pi(x)/f_\pi]$ so that $U(x)=\xi_L^\dagger(x)\xi_R(x)=\exp[2i\pi(x)/f_\pi]$, $\mathcal{L}_A$ reduces to the usual nonlinear-σ-model Lagrangian:

$$\mathcal{L}_A=\frac{f_\pi^2}{4}\mathrm{Tr}(D_\mu U\,D^\mu U^\dagger)\ ,$$

$$D_\mu U=\partial_\mu U-il_\mu U+iUr_\mu\ .$$

The hidden symmetry enables us to add $\mathcal{L}_B$ to $\mathcal{L}_A$ without changing physics described by $\mathcal{L}_A$, since vector-meson fields are just auxiliary fields in the absence of $\mathcal{L}_{\rm kin}(V)$ so that $\mathcal{L}_B$ has no effect on chiral dynamics. A highly nontrivial assumption is that $\mathcal{L}_{\rm kin}(V)$ may be developed by underlying QCD. Even if there is no proof for this assumption in 3+1 dimensions, there are some examples where it is true in lower dimensions [7]. Once we agree to accept this assumption, we can study the dynamical role of vector mesons in strong, electromagnetic and weak interactions of the pion nonet and vector mesons.

In the unitary gauge, the scalar nonet becomes the longitudinal component of the vector meson nonet. By expanding $\xi_L(x)$ and $\xi_R(x)$ in the unitary gauge, setting $l_\mu=r_\mu=eQA_\mu$, and comparing with

$$\mathcal{L}_B=m_V^2\mathrm{Tr}V_\mu^2-2eg_V\mathrm{Tr}V_\mu QA^\mu$$
$$-2ig_{V\pi\pi}\mathrm{Tr}V_\mu[\pi,\partial^\mu\pi]+\cdots\ ,$$

we find that

$$m_V^2=ag^2f_\pi^2,\quad g_V=agf_\pi^2,\quad g_{V\pi\pi}=\tfrac{1}{2}ag\ . \quad (3)$$

(We assume an ideal mixing in the vector-meson sector.) In particular, we have the following relations among g, g_V, and m_V^2 (independent of a):

$$\frac{g_\rho}{m_\rho^2}=\frac{3g_\omega}{m_\omega^2}=\frac{3g_\phi}{\sqrt{2}\,m_\phi^2}=\frac{1}{g}\ . \quad (4)$$

This relation guarantees that vector mesons couple to mesons in a gauge-invariant way. (See Sec. III on $K^+\to\pi^+e^+e^-$, for example.) Instead of the standard chiral perturbation theory based on the loop expansion, which is equivalent to the derivative expansion, we use $\mathcal{L}_{\rm tot}$ with $a=2$. For $a=2$, Eqs. (3) imply the Kawarabayashi-Suzuki-Riazuddin-Fayyazuddin (KSRF) relations [17], the universality [18] of the $V\pi\pi$ couplings ($g_{V\pi\pi}$'s) and $V\gamma$ mixing (g_V's). These are all observed to be approximately true [19] in $V\to\pi\pi$, $V\to\pi\gamma$, the meson mass spectra, and the charge radius of π^+. This would imply that, if we could calculate various properties of low-lying hadrons from the underlying QCD, we would get $a\simeq 2$.

B. Inclusion of the symmetry breaking

One of the phenomenological flaws of the above Lagrangian, Eqs. (1) and (2), is that it does not include symmetry-breaking effects: the explicit chiral-symmetry breaking and the flavor-symmetry breaking. In reality, neither are pions massless, nor are vector mesons degenerate as dictated by Eq. (1).

First of all, chiral symmetry is broken explicitly through the quark masses, as well as spontaneously through the vacuum expectation value of the $q\bar{q}$ condensate. In QCD, the quark mass term transforms as $(3_L,3_R)$ under $\mathrm{U}(3)_L\times\mathrm{U}(3)_R$, so that we may add terms with the same transformation property to Eq. (1). In the lowest order, we choose the following symmetry-breaking term:

$$\mathcal{L}_m=v\,\mathrm{Tr}(mU+U^\dagger m)\ ,$$

where $m=\mathrm{diag}(m_u,m_d,m_s)$ is the quark mass matrix. v is a vacuum expectation value of $\bar{q}q$ representing spontaneous chiral-symmetry breaking. v relates the quark masses with the meson masses in the following way:

$$v=\frac{f_\pi^2m_{\pi^+}^2}{2(m_u+m_d)}=\frac{f_\pi^2m_{K^+}^2}{2(m_u+m_s)}=\frac{f_\pi^2m_{K^0}^2}{2(m_d+m_s)}\ .$$

This gives nonvanishing finite masses to NG bosons. Furthermore, we can easily lift the mass degeneracy of the pion nonet by choosing m not to be proportional to the identity matrix.

Second, we also have to consider the symmetry-breaking effects in the meson decay constants, i.e., $f_K/f_\pi=1.22\neq 1$. We may introduce the symmetry breaking [7] in $\mathcal{L}_A$ as follows:

$$\mathcal{L}'_A=-\frac{f_\pi^2}{4}\mathrm{Tr}\{[(D_\mu\xi_L)\xi_L^\dagger+(D_\mu\xi_L)\epsilon_A\xi_R^\dagger]$$
$$-[(D_\mu\xi_R)\xi_R^\dagger+(D_\mu\xi_R)\epsilon_A\xi_L^\dagger]\}^2\ , \quad (5)$$

where $\epsilon_A=(0,0,c_A)$. By renormalizing the pion nonet field $\pi(x)$ by

$$\pi(x)\to\frac{1}{\sqrt{1+c_A}}\pi(x)\frac{1}{\sqrt{1+c_A}}\ ,$$

we find that $f_K=f_\pi\sqrt{1+c_A}$. This sets $c_A=0.49$. However, we find that it is not easy to make such models consistent with various low-energy data on η,η'

$\rightarrow\gamma\gamma,\pi^+\pi^-\gamma$, for example. Furthermore, calculations based on the effective Lagrangian are not compatible with the current-algebra and PCAC (partial conservation of axial-vector current) calculations.

Third, to achieve the flavor-symmetry breaking in the vector-meson masses, we can modify $\mathcal{L}_B$ in a similar manner as $\mathcal{L}_A$ [6]:

$$\mathcal{L}'_B=-a\frac{f_\pi^2}{4}\mathrm{Tr}\{[(D_\mu\xi_L)\xi_L^\dagger+(D_\mu\xi_L)\epsilon_V\xi_R^\dagger] +[(D_\mu\xi_R)\xi_R^\dagger+(D_\mu\xi_R)\epsilon_V\xi_L^\dagger]\}^2 , \quad (6)$$

where $\epsilon_V=(0,0,c_V)$. Then, Eqs. (3) get modified to

$$m_\rho^2=m_\omega^2=ag^2f_\pi^2=\frac{m_{K^*}^2}{1+c_V}=\frac{m_\phi^2}{(1+c_V)^2} ,$$

$$\frac{g_\rho}{m_\rho^2}=\frac{3g_\omega}{m_\omega^2}=\frac{3g_\phi}{\sqrt{2}\,m_\phi^2}=\frac{1}{g} .$$

From the mass spectrum of vector mesons, we can set $c_V=0.34$. We note that the symmetry-breaking pattern of $\mathcal{L}'_A$ and $\mathcal{L}'_B$ is the same as that of $\mathcal{L}_m$.

To see how well the new Lagrangians, Eqs. (5) and (6), describe meson physics, we calculate the electromagnetic charge radii of π^+, K^+, and K^0. We study this quantity here, since it is the place where the powerfulness of the vector-meson-dominance hypothesis manifests itself, and it is a part of the $K\rightarrow\pi l^+l^-$ process which is the subject of the next section. Define $F_A(s)$ and $G_A(s)$ by

$$\langle A(p')|j_\mu^{\mathrm{em}}|A(p)\rangle =e[(p+p')_\mu F_A(q^2)+(p-p')_\mu G_A(q^2)] ,$$

where $s=q^2=(p-p')^2$. $F_A(0)$ measures the electric charge of the particle A in unit of the electron charge.

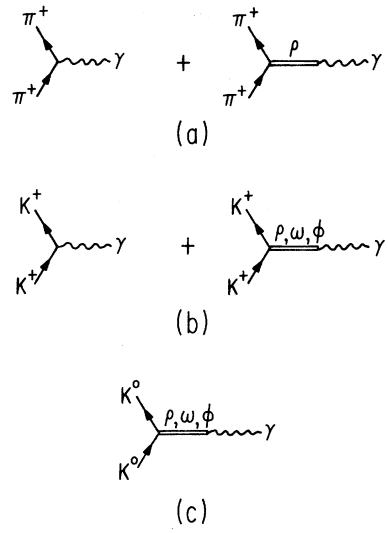

FIG. 1. Feynman diagrams for $\langle P|j_{\mathrm{em}}|P\rangle$ with $P=\pi^+$, K^+, and K^0. The vertices are read off from Eqs. (5) and (6) and their Hermitian conjugates with $a=2$.

For small s, we can expand $F_A(s)$ in Taylor series. The electromagnetic charge radius r_A of the particle A is defined by

$$F_A(s)=1+\frac{s}{6}\langle r_A^2\rangle+\cdots .$$

We first make the Lagrangians Hermitian so that parity and charge-conjugation symmetries are respected. Evaluating the Feynman diagrams shown in Fig. 1, we find

$$F_{\pi^+}(s)=1+\frac{a}{2}[f_\rho(s)-1] ,$$

$$F_{K^+}(s)=1-\frac{c_A}{6}\left[[1-f_\phi(s)]+\frac{2}{1+c_A}[1-\tfrac{3}{4}f_\rho(s)-\tfrac{1}{4}f_\omega(s)]\right] -\frac{a}{6(1+c_A)}\{2(1-c_V)[1-\tfrac{3}{4}f_\rho(s)-\tfrac{1}{4}f_\omega(s)]+(1+c_V)[1-f_\phi(s)]\} ,$$

$$F_{K^0}(s)=-\frac{c_A}{6}\left[[1-f_\phi(s)]-\frac{1}{1+c_A}[1-\tfrac{3}{2}f_\rho(s)+\tfrac{1}{2}f_\omega(s)]\right]+\frac{a}{12}\{(1-c_V)[1-\tfrac{3}{2}f_\rho(s)+\tfrac{1}{2}f_\omega(s)]-(1+c_V)[1-f_\phi(s)]\} ,$$

where

$$f_V(s)=\frac{m_V^2}{m_V^2-s} .$$

From the above equations, we note that there is no direct $\pi\pi\gamma$ coupling for any c_A and c_V if we set $a=2$. For K^+, this is true only if $c_A=c_V=0$. The numerical values for $\langle r_A^2\rangle$ are given in Table I for $a=2$ (complete vector-meson dominance). We find that an acceptable fit to the experimental data [20,21] is obtained if we put $c_A=c_V=0$ and still insist on using the physical masses for vector mesons, which is the most naive case. Then, we can freely use the KSRF relation and Eq. (4) to express g and g_V in terms of m_V^2 and f_π^2. This is the same as the form used in the old current-field identity:

$$J_\mu^{\mathrm{vector}}=-2gf_\pi^2V_\mu+\cdots=-\frac{m_V^2}{f_V}V_\mu+\cdots .$$

TABLE I. The squares of electromagnetic charge radii of π^+, K^+, and K^0 (in units of fm^2) for different values of c_A and c_V obtained from the Lagrangians $\mathcal{L}'_A$ and $\mathcal{L}'_B$, Eqs. (5) and (6). The data are taken from Ref. [20] for π^+ and K^+ and from Ref. [21] for K^0.

(c_A,c_V)	(0,0)	(0,0.34)	(0.49,0)	(0.49,0.34)	Expt. data
π^+	0.39	0.39	0.39	0.39	0.439±0.03
K^+	0.34	0.27	0.28	0.24	0.28±0.07
K^0	−0.028	+0.0056	−0.049	+0.0001	−0.054±0.026

$c_A=0.49$ and $c_V=0$ are not considered in this paper for simplicity.

We also note that the charge radius of π^+ is a little smaller than the actual value. This could be remedied if we used a smaller value of $m_\rho \simeq 730$ MeV. This can be understood in the following way: we regarded the ρ meson as a fundamental pointlike particle in our formalism. In actuality, this is not true, and ρ should be considered as a resonance with $\pi\pi$ scattered in the $I=J=1$ state. The constraints from current algebra, unitarity, and crossing symmetry can be approximately implemented, and one obtains a modified ρ meson form factor [22]. However, such works have not been done yet for ω and ϕ. So, we ignore such complications arising from the composite nature of vector mesons hereafter, and regard Eqs. (1) and (2) as the basic Lagrangians for our purposes. Also, we will freely use Eq. (3) in the following.

C. The Wess-Zumino anomaly in the absence of vector mesons

The Lagrangian in Eqs. (1) and (2) without Γ^{anom} has a spurious symmetry (intrinsic parity, P_0 [23]) which is not a true symmetry of underlying physics of QCD [24]. The famous Wess-Zumino (WZ) anomaly [25] removes this symmetry, and gives a consistent explanation for intrinsic parity- (P_0-) violating processes such as $\pi^0\to\gamma\gamma$, $\gamma\to 3\pi$, $K^+K^-\to 3\pi$, etc. Furthermore, the amplitudes for those P_0-violating processes are related to each other in the chiral limit, forming another set of low-energy theorems. Hence, the WZ term is indispensable to describe the chiral dynamics of the lowest-lying mesons. At the quark level, the anomaly is a manifestation of the fact that one cannot retain chiral symmetry in the quantized theory of fermions coupled to gauge fields [26]. This fact is reflected in the gauge transformation property of the effective action: in the presence of the anomaly, the effective action is not gauge invariant, and the current is not conserved [26–31].

The explicit form of the anomaly in the absence of vector mesons can be derived in various ways. The key point is to construct a functional, $\Gamma(U=\xi_L^\dagger\xi_R, l_\mu, r_\mu)$, which transforms under the local $G=\mathrm{U}(3)_L\times\mathrm{U}(3)_R$ as

$$\delta\Gamma_{\mathrm{LR}}(U,l,r) = -\frac{N_c}{24\pi^2}\int_{M^4} d^4x \left[\epsilon_L\left[(dl)^2-\frac{i}{2}dl^3\right]-(L\to R)\right], \tag{7}$$

which is the result of the calculation at the quark level [28]. (N_c is the number of colors of the quarks.) This is the anomaly-matching condition at the fundamental level and the constituent level. The explicit form can be conveniently written in terms of the language of differential forms [27]:

$$\Gamma_{LR}=C\int_{M^5} d^5x\ \mathrm{Tr}\alpha^5+(\text{covariantization}),$$

where we define

$$\alpha=dU\,U^{-1},\quad \beta=U^{-1}dU,\quad C=-i\frac{N_c}{240\pi^2}. \tag{8}$$

α and β transform as $\mathrm{U}(3)_L$ and $\mathrm{U}(3)_R$ nonets respectively under the global $G=\mathrm{U}(3)_L\times\mathrm{U}(3)_R$. To begin with, consider the gauge transformation property of $\mathrm{Tr}(\alpha^5)$. Under local $G=\mathrm{U}(3)_L\times\mathrm{U}(3)_R$ transformations,

$$\delta U(x)=i[\epsilon_L(x)U(x)-U(x)\epsilon_R(x)],$$

$$\delta l(x)=d\epsilon_L(x)+i[\epsilon_L(x),l(x)],$$

$$\delta r(x)=d\epsilon_R(x)+i[\epsilon_R(x),r(x)],$$

it changes by

$$C\delta\int_{M^5} d^5x\ \mathrm{Tr}(\alpha^5)=-5Ci\int_{M^4} d^4x\ \mathrm{Tr}(d\epsilon_L\alpha^3+d\epsilon_R\beta^3). \tag{9}$$

This can be removed by introducing the term

$$5Ci\int_{M^4} d^4x\ \mathrm{Tr}(l\alpha^3+r\beta^3),$$

whose gauge-transformation property is

$$\begin{aligned}5Ci\delta\int_{M^4} d^4x\ \mathrm{Tr}(l\alpha^3+r\beta^3)=&5Ci\int_{M^4} d^4x\ \mathrm{Tr}(d\epsilon_L\alpha^3+d\epsilon_R\beta^3)+5C\int_{M^4} d^4x\ \mathrm{Tr}[d\epsilon_L(l\alpha^2-\alpha l\alpha+\alpha^2 l)]\\&-5C\int_{M^4} d^4x\ \mathrm{Tr}[d\epsilon_R(r\beta^2-\beta r\beta+\beta^2 r)]\\&+5C\int_{M^4} d^4x\ \mathrm{Tr}[d\epsilon_L(UrU^{-1}\alpha^2-\alpha UrU^{-1}\alpha+\alpha^2 UrU^{-1})]\\&-5C\int_{M^4} d^4x\ \mathrm{Tr}[d\epsilon_R(U^{-1}lU\beta^2-\beta U^{-1}lU\beta+\beta^2U^{-1}lU)].\end{aligned} \tag{10}$$

We note that Eq. (9) is canceled by the first term of the right-hand side of Eq. (10). However, there are remaining terms in Eq. (10) which are not equal to the anomaly condition, Eq. (7). Therefore, we proceed as before by adding terms whose gauge transformations are canceled by the remainders in Eq. (10), and so on, until we end up with Eq. (7). The final result is

$$\Gamma_{LR}(U,l_\mu,r_\mu)=C\int_{M^5}d^5x\ \mathrm{Tr}(\alpha^5)$$
$$+5C\int_{M^4}d^4x\ \mathrm{Tr}\{i(l\alpha^3+r\beta^3)-[(dl\,l+l\,dl)\alpha+(dr\,r+r\,dr)\beta]+(dl\,dU\,rU^{-1}-dr\,dU^{-1}lU)$$
$$+(rU^{-1}lU\beta^2-lUrU^{-1}\alpha^2)+\tfrac{1}{2}[(l\alpha)^2-(r\beta)^2]+i[l^3\alpha+r^3\beta]$$
$$+i[(dr\,r+r\,dr)U^{-1}lU-(dl\,l+l\,dl)UrU^{-1}]+i[lUrU^{-1}l\alpha+rU^{-1}lUr\beta]\,.$$
$$+[r^3U^{-1}lU-l^3UrU^{-1}+\tfrac{1}{2}(UrU^{-1}l)^2]\}\,, \tag{11}$$

where M^5 is a five-dimensional manifold whose boundary is the ordinary Minkowski manifold M^4. This $G=\mathrm{U}(3)_L\times\mathrm{U}(3)_R$-invariant form of the anomaly was used in the original paper by Fujiwara *et al.* [29]. However, this form of the anomaly is not consistent with current algebra and modified PCAC in the following sense. From the above Lagrangian, Eq. (1), we can construct the left-handed and the right-handed currents $j_{L\mu}$ and $j_{R\mu}$. Then, we find that the axial-vector current J_μ^{axial} is given by

$$J_\mu^{\mathrm{axial}}(x)=-f_\pi D_\mu\pi(x)-\frac{\alpha}{\pi f_\pi}\epsilon_{\mu\nu\alpha\beta}Q^2A^\nu(x)\partial^\alpha A^\beta(x)\,.$$

If we take the divergence of $J_\mu^{\mathrm{axial}}(x)$ and use the Euler-Lagrange equation for $\pi(x)$ derived from Eq. (1), we can show that the axial-vector current for the third component of the isospin, $A_\mu^{3,\mathrm{axial}}$, satisfies

$$\partial^\mu J_\mu^{3,\mathrm{axial}}(x)=f_\pi m_{\pi^0}^2\phi_{\pi^0}(x)$$
$$+(1-\tfrac{1}{3})\frac{\alpha}{\pi f_\pi}\epsilon_{\mu\nu\alpha\beta}\partial^\mu A^\nu(x)\partial^\alpha A^\beta(x)\,,$$

where $\phi_{\pi^0}(x)$ is an interpolating pion field appearing in the calculation in the Lehmann-Symanzik-Zimmermann (LSZ) formalism. This is not consistent with the modified PCAC relation [30] which has the coefficient 1 in front of Q^2 instead of $(1-\frac{1}{3})=\frac{2}{3}$. This in turn means that we get too small a rate for $\pi^0\to\gamma\gamma$ when it is calculated by the current algebra and the modified PCAC in the LSZ formalism. To keep the consistency between the effective-Lagrangian approach and the good old current-algebra and PCAC calculation of $\pi^0\to\gamma\gamma$ in the LSZ formalism, we should modify the LR-symmetric anomaly form, Eq. (11). The correct answer is to keep the conservation of vector currents, sacrificing that of axial-vector currents as done by Bardeen [31]. Bardeen's form of the anomaly satisfies the following condition under the local $G=\mathrm{U}(3)_L\times\mathrm{U}(3)_R$:

$$\delta\Gamma_{\mathrm{WZ}}(U,l,r)=\frac{3N_c}{24\pi^2}\int d^4x\left[(\epsilon_L-\epsilon_R)\left[F_{\mathcal{V}}^2+\frac{1}{3}F_{\mathcal{A}}^2-\frac{4i}{3}(F_{\mathcal{V}}\mathcal{A}^2+\mathcal{A}F_{\mathcal{V}}\mathcal{A}+\mathcal{A}^2F_{\mathcal{V}})-\frac{8}{3}\mathcal{A}^4\right]\right]\,, \tag{12}$$

where

$$\mathcal{V}=\tfrac{1}{2}(l+r),\quad \mathcal{A}=\tfrac{1}{2}(l-r)\,,$$
$$F_{\mathcal{V}}=d\mathcal{V}+i(\mathcal{V}^2+\mathcal{A}^2)\,,$$
$$F_{\mathcal{A}}=d\mathcal{A}+i(\mathcal{V}\mathcal{A}+\mathcal{A}\mathcal{V})\,.$$

For the vector transformation, $\epsilon_L=\epsilon_R$, and the above anomaly vanishes identically. This in turn ensures the conservation of the vector currents, as we anticipated.

The minimal solution to this equation is given simply in terms of $\Gamma_{LR}(U,l,r)$ as

$$\Gamma_{\mathrm{WZ}}(U,l,r)=\Gamma_{LR}(U,l,r)-\Gamma_{LR}(U=1,l,r)\,. \tag{13}$$

This coincides with the original form of Wess and Zumino. If we consider only electromagnetic fields as external gauge fields, we have $l_\mu=r_\mu=eQA_\mu$. Since $\Gamma_{LR}(U=1,l,r)$ is antisymmetric under $l\leftrightarrow r$, the two forms of anomalies, Γ_{LR} and Γ_{WZ} are identical.

D. The WZ anomaly in the presence of vector mesons

Electromagnetic decays of vector mesons such as $\omega\to\pi^0\gamma$, $\omega\to\rho\pi$, etc., are all intrinsic parity-violating processes, so that we might be able to describe them in the effective-Lagrangian approach by including terms with the Levi-Civita tensor. One can achieve this by adding homogeneous solutions of Eq. (12) to Eq. (13). Since the newly added terms are homogeneous solutions of the anomaly equation (i.e., gauge invariant, or $\delta\Gamma=0$), there will be no additional anomaly and the anomalous low-energy theorems remain intact.

The correct form of the WZ anomaly including vector mesons is conveniently expressed in terms of the following gauge-covariant entities [29]:

$$\hat{\alpha}_L=D\xi_L\cdot\xi_L^\dagger=\alpha_L-igV+i\hat{l}\,,$$
$$\hat{\alpha}_R=D\xi_R\cdot\xi_R^\dagger=\alpha_R-igV+i\hat{r}\,,$$
$$\alpha_{L(r)}=d\xi_{L(R)}\cdot\xi_{L(R)}^\dagger\,,$$
$$\hat{l}=\xi_L\cdot l\cdot\xi_L^\dagger,\quad \hat{r}=\xi_R\cdot r\cdot\xi_R^\dagger\,, \tag{14}$$
$$F_V=dV-igV^2\,,$$
$$\hat{F}_L=\xi_L\cdot F_L\cdot\xi_L^\dagger=\xi_L(dl-il^2)\xi_L^\dagger\,,$$
$$\hat{F}_R=\xi_R\cdot F_R\cdot\xi_R^\dagger=\xi_R(dr-ir^2)\xi_R^\dagger\,.$$

There are four gauge invariants [i.e., homogeneous solutions of the anomaly condition, Eq. (12)] which conserve parity and charge conjugation but violate intrinsic parity, since they contain the Levi-Civita tensor:

$$\begin{aligned}
&\mathcal{L}_1=\mathrm{Tr}(\hat{\alpha}_L^3\hat{\alpha}_R-\hat{\alpha}_R^3\hat{\alpha}_L)-(\xi_L=\xi_R=1,\ V=0,l,r)\ ,\\
&\mathcal{L}_2=\mathrm{Tr}(\hat{\alpha}_L\hat{\alpha}_R\hat{\alpha}_L\hat{\alpha}_R)-(\xi_L=\xi_R=1,\ V=0,l,r)\ ,\\
&\mathcal{L}_3=i\,\mathrm{Tr}F_V(\hat{\alpha}_L\hat{\alpha}_R-\hat{\alpha}_R\hat{\alpha}_L)-(\xi_L=\xi_R=1,\ V=0,l,r)\ ,\\
&\mathcal{L}_4=i\,\mathrm{Tr}(\hat{F}_L\hat{\alpha}_L\hat{\alpha}_R-\hat{F}_R\hat{\alpha}_R\hat{\alpha}_L)-(\xi_L=\xi_R=1,\ V=0,l,r)\ .
\end{aligned}\tag{15}$$

Here, the second term means the same expression as the first term evaluated at $\xi_L=\xi_R=1$, $V=0$. The general solutions to the anomaly equation, Eq. (12), are the Wess-Zumino term, Eq. (13), and any linear combinations of the above $\mathcal{L}_{1-4}(\xi_L,\xi_R,V,l,r)$:

$$\Gamma^{\mathrm{anom}}=\Gamma_{\mathrm{WZ}}+\sum_{i=1}^{4}c_i\mathcal{L}_i\ .$$

The coefficients c_i's are to be determined by fitting the data on $\pi^0\to\gamma\gamma$, $\omega\to\pi^0\gamma$, etc. In particular,

$$\Gamma^{\mathrm{anom}}=\Gamma_{\mathrm{WZ}}-15C(\mathcal{L}_3+\mathcal{L}_4+c_1\mathcal{L}_1+c_2\mathcal{L}_2)|_{c_1-c_2=-1}\ ,\tag{16}$$

contains $VV\pi$ and $\gamma\pi^3$ vertices, and there is no direct $\pi\gamma\gamma$ coupling. Therefore, complete vector-meson dominance (VMD) is not realized in $\gamma\pi^3$ vertices. The $\pi^0\to\gamma\gamma$ process is described by $\pi\to\omega\rho\to\gamma\gamma$ through the $V\gamma$ mixing, $\omega,\rho\to\gamma$. The first comes from Eq. (16), and the second from Eq. (2). Also, our choice $c_1-c_2=-1$ gives the right value for $\omega\to3\pi$ [29]. From Eq. (16), we get $\Gamma(\omega\to3\pi)=9.1$ MeV compared with the experimental value, 8.9 ± 0.3 MeV. If we chose $c_1-c_2=+1$ in Eq. (16), we would have complete vector-meson dominance in $V\pi^3$; i.e., there would be no direct $\gamma\pi^3$ vertices. This also would lead to $\Gamma(\omega\to3\pi)=6.1$ MeV, which is about 70% of the observed rate. We can easily read off the $VV\pi$ and $V\pi\gamma$ vertices from this Lagrangian, Eq. (16). Before closing this subsection, we emphasize that our discussions in the remaining of this paper do not depend on the specific value of c_1-c_2, since $\mathcal{L}_1$ and $\mathcal{L}_2$ do not contribute any processes we are concerned with.

III. THE STRUCTURE OF THE $|\Delta S|=1$ WEAK LAGRANGIAN

A. The structure of the left-handed currents

To study nonleptonic decays of kaons, we need the left-handed current in terms of meson fields. We can construct currents either by the Noether method or by taking the functional derivative of the effective action with respect to gauge fields l_μ and then setting $l_\mu=r_\mu=eQA_\mu$. Since our Lagrangian is already written in a fully gauged form, we use the second method. We put superscripts to the currents to identify from which Lagrangian the current is constructed. Also, we sometimes denote the field content of the current in the parentheses. For example, $j_L^{\mathrm{WZ}}(\pi\gamma)$ will indicate that the current is constructed from the Wess-Zumino anomaly and that it couples to the pion nonet and a photon.

We first give the currents from $\mathcal{L}_A$ and $\mathcal{L}_B$:

$$\begin{aligned}
j_{L\mu}^A&=-f_\pi D_\mu\pi-i[\pi,D_\mu\pi]\ ,\\
j_{L\mu}^B&=\frac{ia}{2}[\pi,D_\mu\pi]-af_\pi^2(gV_\mu-eQA_\mu)\\
&\quad-iaf_\pi[\pi,gV_\mu-eQA_\mu]\ ,
\end{aligned}\tag{17}$$

We note that the π^2 terms in j_L^A and j_L^B cancel each other if we set $a=2$ (VMD). Higher-order terms irrelevant to our purposes are not shown here. We note that our model is different from the previous calculations using current-field identities, which do not contain the $[\pi,gV_\mu-eQA_\mu]$ term. This term generates *weak* $V\pi\pi$ vertices.

Most important is the anomalous current from the anomaly:

$$\Gamma^{\mathrm{anom}}(U,l,r,V)=\Gamma_{\mathrm{WZ}}(U,l,r)+\Gamma_V^{\mathrm{anom}}(\xi_L,\xi_R,l,r,V)\ .\tag{18}$$

In the absence of vector mesons, $\Gamma_V^{\mathrm{anom}}=0$ so that only $\Gamma_{\mathrm{WZ}}(U,l,r)$ will contribute to the anomalous left-handed current. So, we first consider j_L^{WZ}. (For the anomaly and the anomalous currents, we use the notation of differential forms for simplicity.) By setting $l=eQA+W$ in Eq. (16) and reading off the coefficients of W, we find that

$$j_L^{\mathrm{WZ}}(\pi\gamma)=\frac{30Cie}{f_\pi}\{d\pi,Q\,dA\}\ .\tag{19}$$

There are other pieces involving π^3, $\pi^2\gamma$, $\pi\gamma^2$, etc., which are irrelevant to our study of $K_L\to\gamma l^+l^-$ and $K_L\to\pi^0\gamma\gamma$.

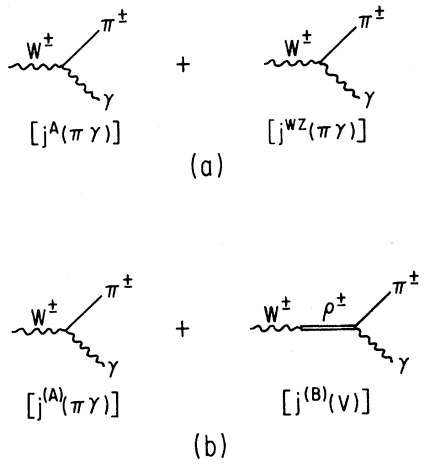

FIG. 2. Feynman diagrams for $W^+\to\pi^+\gamma$ in our model: (a) in the absence of vector mesons; (b) in the presence of vector mesons.

If we neglected vector mesons completely, this would be the whole story, and the weak vertices from $j_L^{WZ}(\pi\gamma)$ and other normal currents, j_L^A and j_L^B, should be able to describe nonleptonic decays of kaons such as $K_L\to\gamma e^+e^-$, $K_L\to\pi^0\gamma\gamma$ and so on, in which anomalies take part. In this case, we will find that we plunge into disagreements between the theoretical predictions and the experimental data.

For example, the above $j_L^{WZ}(\pi\gamma)$ current can make a real W boson decay into $\pi\gamma$ with a large branching ratio. [See Fig. 2(a).] Our calculation is nothing but the calculation done in Ref. [32] in a different language. They used the triangle anomaly and PCAC, while we are using the effective-Lagrangian method with the anomaly properly taken into account. Of course, it is not sensible to use the effective Lagrangian when one of the external particles has a huge mass compared to the chiral-symmetry-breaking scale. The calculated number should not be taken too seriously. However, we discuss it to demonstrate that vector mesons cut off the bad high-energy behavior of the chiral amplitude. This phenomenon was observed in $\gamma\gamma\to\pi^0\pi^0$ [5], and we will find a similar situation when we discuss $K_L\to\pi^0\gamma\gamma$ (see Secs. VI B and VI C.)

From the above current or the gauged Wess-Zumino anomaly, Eq. (11), we find that

$$\mathcal{M}^{(a)}(W(P,\epsilon)\to\pi\gamma(k,\epsilon'))=-\frac{2\pi\alpha f_\pi\cos\theta_C}{\sin\theta_W}\left[\epsilon\cdot\epsilon'+\frac{i}{8\pi^2f_\pi^2}\epsilon^{\mu\nu\alpha\beta}k_\mu\epsilon'_\nu P_\alpha\epsilon_\beta\right], \tag{20}$$

where the first term in the large parentheses comes from the normal current j_L^A, and is negligible compared to the second term. This leads to the branching ratio $\Gamma(W\to\pi\gamma)\simeq 1.3\Gamma(W\to e\nu)$. Note that a recent measurement [33] reports $\Gamma(W\to\pi\gamma)<5.8\times10^{-2}\ \Gamma(W\to e\nu)$.

Let us see what happens if we include vector mesons. $\Gamma_V^{\rm anom}$ generates the new pieces of currents relevant to our discussions of $W\to\pi\gamma$, $K_L\to\gamma l^+l^-$, and $K_L\to\pi^0\gamma\gamma$:

$$j_L^V(\pi\gamma)=\frac{30Cie}{f_\pi}\{d\pi,Q\,dA\}\ , \tag{21}$$

$$j_L^V(V\gamma)=30Cie\{gV-eQA,Q\,dA\}\ . \tag{22}$$

The total anomalous current is the sum of j_L^{WZ} and j_L^V:

$$j_L^{\rm anom}(\pi\gamma)=j_L^{WZ}(\pi\gamma)+j_L^V(\pi\gamma)=0\ , \tag{23}$$

$$j_L^{\rm anom}(V\gamma)=30Cie\{gV-eQA,Q\,dA\}\ . \tag{24}$$

Therefore, the second term in $\mathcal{M}^{(a)}(W\to\pi\gamma)$ becomes zero. In the presence of vector mesons, we have an additional diagram [Fig. 2(b)]. We can easily evaluate it using Eqs. (1) and (16), and the result is

$$\mathcal{M}^{(b)}(W(P,\epsilon)\to\pi\gamma(k,\epsilon'))=-\frac{2\pi\alpha f_\pi\cos\theta_C}{\sin\theta_W}\left[\epsilon\cdot\epsilon'+\frac{i}{8\pi^2f_\pi^2}\frac{m_\rho^2}{m_\rho^2-M_W^2}\epsilon^{\mu\nu\alpha\beta}k_\mu\epsilon'_\nu P_\alpha\epsilon_\beta\right], \tag{25}$$

corresponding to $\Gamma(W\to\pi\gamma)\simeq 9.9\times10^{-8}\Gamma(W\to e\nu)$. This should be compared with the more refined calculations [34] based on QCD, $B(W\to\pi\gamma)\simeq 3\times10^{-8}\Gamma(W\to e\nu)$. This analysis may be taken as one piece of evidence that the inclusion of vector mesons is very important to control the high-energy behavior of chiral amplitudes. In passing, we remark that $j_L^{\rm anom}(V\gamma)$ will give very important contributions to $K_L\to\gamma l^+l^-$ and $K_L\to\pi^0\gamma\gamma$ (see Secs. V and VI). Also, it should be emphasized that (i) Eqs. (21) and (23) are the result of choosing c_3 and c_4 as in Eq. (16), i.e., complete vector-meson dominance in $\pi\gamma\gamma$, or no direct $\pi\gamma\gamma$ coupling as described at the end of the previous subsection, and (ii) $\mathrm{Tr}[j_L^{\rm anom}(\pi\gamma)]$ and $\mathrm{Tr}[j_L^{\rm anom}(V\gamma)]$ are nonvanishing even in the case of $SU(3)_L\times SU(3)_R$, in sharp contrast to $\mathrm{Tr}(D_\mu\pi)$. The second property, (ii), turns out to be very important in $K_L\to\gamma l^+l^-$ and $K_L\to\pi^0\gamma\gamma$.

Finally, we comment on the influence of choosing Bardeen's form of the anomaly instead of the left-right-symmetric form. If we chose the left-right-symmetric form, we would have

$$j_L^{\rm anom}(\gamma\gamma)=-10Cie^2\{QA,Q\,dA\}\ .$$

This would contribute to $K_L\to\gamma\gamma$, $K_L\to\gamma l^+l^-$, for example. Although there is no definite restriction on such a current from experiments, it can be excluded by the arguments given in Sec. II C: We should keep vector currents conserved, sacrificing the conservation of axial-vector currents to get the right value for $\pi^0\to\gamma\gamma$ in the LSZ formalism with modified PCAC.

B. The $|\Delta S|=1$ weak Lagrangian for nonleptonic decays of kaons

To study nonleptonic decays of kaons, we assume that the effective weak Lagrangian has the following form in terms of the $U(3)_L$ left-handed current $j_{L\mu}$ constructed from the Lagrangian, Eq. (1):

$$\mathcal{L}_{\text{weak}}^{\Delta S=1}=\mathcal{L}_{(8,1)}^{\Delta I=1/2}+\mathcal{L}_{(27,1)}^{\Delta I=1/2}+\mathcal{L}_{(27,1)}^{\Delta I=3/2}\ , \tag{26}$$

$$\mathcal{L}_{(8,1)}^{\Delta I=1/2}=\frac{C_8^{(1/2)}G_F}{\sqrt{2}}\{\mathrm{Tr}(j_{\mu L}j_L^{\mu}\lambda_6)-\delta_p[(j_{\mu L})_{23}+(j_{\mu L})_{32}]\mathrm{Tr}(j_L^{\mu})\}\ , \tag{27}$$

$$\mathcal{L}_{(27,1)}^{\Delta I=1/2}=\frac{C_{27}^{(1/2)}G_F}{\sqrt{2}}\{(j_{\mu L})_{13}(j_L^{\mu})_{21}+(j_{\mu L})_{31}(j_L^{\mu})_{12}+\tfrac{1}{2}[(j_{\mu L})_{23}+(j_{\mu L})_{32}][9(j_{11L}^{\mu}+j_{22L}^{\mu})-(j_{11L}^{\mu}-j_{22L}^{\mu})-6\,\mathrm{Tr}(j_L^{\mu})]\}, \tag{28}$$

$$\mathcal{L}_{(27,1)}^{\Delta I=3/2}=\frac{C_{27}^{(3/2)}G_F}{\sqrt{2}}\{(j_{\mu L})_{13}(j_L^{\mu})_{21}+(j_{\mu L})_{31}(j_L^{\mu})_{12}+[(j_{\mu L})_{23}+(j_{\mu L})_{32}][j_{L11}^{\mu}-j_{L22}^{\mu}]\}\ . \tag{29}$$

Comparing with the usual expressions for the $SU(3)_L$ case [35], our expressions have additional terms containing $\mathrm{Tr}(j_L^{\mu})$, i.e., our expressions get reduced to the conventional expressions for the $SU(3)_L\times SU(3)_R$ case if we set $\mathrm{Tr}(j_L^{\mu})=0$. In the previous subsection, however, we have observed that $\mathrm{Tr}(j_{L\mu}^{\text{anom}})\neq 0$ even for the $SU(3)_L\times SU(3)_R$ case. Therefore, we should not drop terms containing $\mathrm{Tr}(j_L^{\mu})$. Since the trace of normal currents is at best proportional to $\partial_\mu\eta_0$, these new terms do not affect the processes such as $K\to 2\pi$, 3π, etc. If we work with the $SU(3)_L\times SU(3)_R$ chiral Lagrangian without vector mesons, the process $K_L\to\pi^0\gamma\gamma$ is the first place where we can see the effect of δ_p and $\mathrm{Tr}[j_{L\mu}^{\text{anom}}(\pi\gamma)]$. (See Sec. VI B for details.) If we work with the $U(3)_L\times U(3)_R$ chiral Lagrangian with or without vector mesons, the decay modes $K_L\to\gamma\gamma$ and $K_L\to\gamma l^+l^-$ are also affected by these new terms.

To understand the above weak Lagrangians with $\mathrm{Tr}(j_L)\neq 0$, we consider the $|\Delta S|=1$ effective Lagrangian in terms of quark fields. It is well known that [9,10]

$$\mathcal{L}_{\text{weak}}^{\Delta S=1}=\sum_{i=1}^{6}b_i(\mu)O_i(\mu)+\text{H.c.}\ ,$$

$$O_1=(\bar{s}u)_{V-A}(\bar{u}d)_{V-A}-(\bar{s}d)_{V-A}(\bar{u}u)_{V-A}\ ,$$

$$O_2=2(\bar{s}d)_{V-A}(\bar{q}q)_{V-A}+O_1\ ,$$

$$O_3=(\bar{s}d)_{V-A}(\bar{u}u)_{V-A}+(\bar{s}u)_{V-A}(\bar{u}d)_{V-A}+2(\bar{s}d)_{V-A}(\bar{d}d)_{V-A}-3(\bar{s}d)_{V-A}(\bar{s}s)_{V-A}\ ,$$

$$O_4=(\bar{s}d)_{V-A}(\bar{u}u)_{V-A}+(\bar{s}u)_{V-A}(\bar{u}d)_{V-A}-(\bar{s}d)_{V-A}(\bar{d}d)_{V-A}\ ,$$

$$O_5=(\bar{s}d)_{V-A}(\bar{q}q)_{V+A}\ ,$$

$$O_6=-8(\bar{s}_Lq_R)(\bar{q}_Ld_R)\ .$$

Here, $(\bar{q}^jq^i)_{V-A}\equiv\bar{q}^j\gamma^\mu(1-\gamma_5)q^i$ and $q_{R(L)}=\frac{1}{2}(1\pm\gamma_5)q$, where $\bar{q}\equiv(\bar{u},\bar{d},\bar{s})$. Our definitions of O_i's are identical with those of Ref. [9], except that the sign of O_1 is changed and O_5 and O_6 are switched. Typical values of b_i's are $b_1=2.5$, $b_2=0.09$, $b_3=0.08$, $b_4=5b_3=0.44$, $b_5=-0.015$ and $b_6=-0.066$ at the hadronic scale [9].

We identify the $(V-A)$ current of quark fields with the left-handed current of meson fields by setting $(\bar{q}^jq^i)_{V-A}=2(j_L)_{ij}$ [36]. Then, the operator O_1, which has the largest Wilson coefficient b_1 and transforms as $\Delta I=\frac{1}{2}$ $(8_L,1_R)$, becomes

$$\begin{aligned}O_1&=(\bar{s}u)_{V-A}(\bar{u}d)_{V-A}-(\bar{s}d)_{V-A}(\bar{u}u)_{V-A}\\&\propto(j_{L\mu})_{13}(j_L^{\mu})_{21}-(j_{L\mu})_{23}(j_L)_{11}^{\mu}\\&=(j_{L\mu}j_L^{\mu})_{23}-(j_{L\mu})_{23}\mathrm{Tr}(j_L^{\mu})\ .\end{aligned}$$

If we take the sum of O_1 and its Hermitian conjugate, we end up with Eq. (27) with $\delta_p=1$. The other two equations, Eqs. (28) and (29), can be derived from chiral representations of O_3 and O_4 in a similar manner. O_3 and O_4 transform as $(27_L,1_R)$ with $\Delta I=\frac{1}{2}$ and $\frac{3}{2}$ respectively, while the other four operators transform as $(8_L,1_R)$ with $\Delta I=\frac{1}{2}$. Therefore, O_3 and O_4 do not mix with other operators under QCD corrections, and their Wilson coefficients, b_3 and b_4 retain the relation $b_4=5b_3$ [9]. Therefore, we set $C_{27}^{(3/2)}=5C_{27}^{(1/2)}$ in Eqs. (28) and (29). The operator O_2 becomes

$$O_2\propto(j_{L\mu}j_L^{\mu})_{23}+(j_{L\mu})_{23}\mathrm{Tr}(j_L^{\mu})\ .$$

The operator O_5 becomes

$$[(j_{L\mu})_{23}+(j_{L\mu})_{23}]\mathrm{Tr}(j_R^{\mu})\ .$$

Since its Wilson coefficient b_5 is smaller than others for operators with $\Delta I=\frac{1}{2}$, we will ignore this term. O_6 can be shown to have a similar form as O_1 if factorization holds [37]. Therefore, the $\Delta I=\frac{1}{2}$, $(8_L,1_R)$ piece can be written as Eq. (27) with an arbitrary parameter δ_p, which is a combination of b_1, b_2, and b_6. Note that $\delta_p=1$ if we have O_1 only. (δ_p-1) measures the contributions of other operators than O_1 to $\Delta I=\frac{1}{2}$ amplitudes. In the $1/N_c$ approach, the leading term has a single trace over the flavor indices [36], and the term with δ_p is suppressed with respect to the usual term, $\mathrm{Tr}(j_{L\mu}j_L^{\mu}\lambda_6)$. This amounts to setting $\delta_p=0$ in the leading order in the $1/N_c$ expansion. This is possible since the two terms in Eq. (27) separately have the right chiral transformation property. On the other hand, if we assume that the $\mathrm{Tr}(j_{L\mu})$ term is suppressed with respect to other terms in Eq. (28) and drop it, the remainder does not have the right chiral transformation property. Based on the $1/N_c$ expansion argument, we expect δ_p to be rather small. We find that this is true from the analyses in Secs. V and VI.

In this paper, we assume *CP* invariance, so that the coefficients C's in Eqs. (27)–(29) are real. Therefore, there appear three independent unknown parameters

$C_8^{(1/2)}$, $C_{27}^{(1/2)}$, $C_{27}^{(3/2)}=5C_{27}^{(1/2)}$ and δ_p at the weak-interaction level.

C. Determination of C's from $K\to\pi\pi$

To fix those parameters, we consider $K_1\to\pi^+\pi^-$, $K_1\to\pi^0\pi^0$, and $K^+\to\pi^+\pi^0$. The relevant Feynman diagrams are shown in Fig. 3. There would be no direct $K\pi\pi$ weak coupling, because we set $a=2$. The invariant matrix elements are

$$\mathcal{M}(K_1\to\pi^+\pi^-)$$
$$=\frac{iG_Ff_\pi}{4\sqrt{2}}(C_8^{(1/2)}+C_{27}^{(1/2)}+C_{27}^{(3/2)})(2P_K^2-p_+^2-p_-^2)\ ,$$
$$\mathcal{M}(K_1\to\pi^0\pi^0)$$
$$=\frac{iG_Ff_\pi}{4\sqrt{2}}(C_8^{(1/2)}+C_{27}^{(1/2)}-2C_{27}^{(3/2)})(2P_K^2-2p_0^2)\ ,$$
$$\mathcal{M}(K^+\to\pi^+\pi^0)=\frac{iG_Ff_\pi}{4\sqrt{2}}(3C_{27}^{(3/2)})(P_K^2-p_\pi^2)\ . \tag{30}$$

It is amusing to observe that we recover the same results one would get from the lowest-order chiral perturbation theory without vector mesons. This is the result of our use of the KSRF relation: we have used Eq. (3) to replace $2g^2f_\pi^2$ by $m_{K^*}^2$. We can calculate the decay width for each process from the above amplitudes, and compare with the experimental data [38] using

$$\Gamma(K\to\pi\pi)=\frac{1}{8\pi}|\mathcal{M}(K\to\pi\pi)|^2\frac{|\mathbf{p}_\pi|}{m_K^2}\ .$$

First of all, we can easily find that $C_{27}^{(3/2)}=0.14$ from the observed $K^+\to\pi^+\pi^0$ rate. But this value of $C_{27}^{(3/2)}$ is not consistent with two equations we get from K_1 decays. Specifically, we have

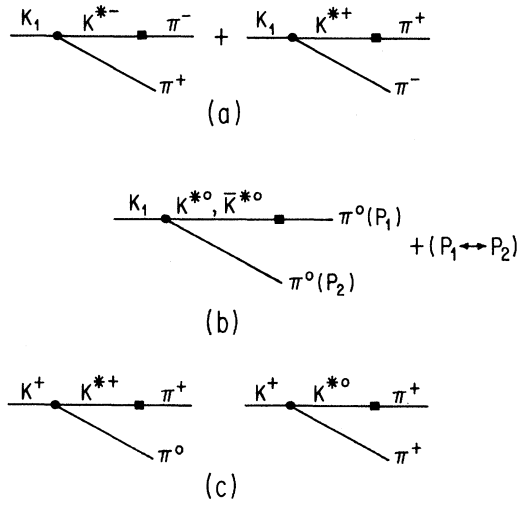

FIG. 3. Feynman diagrams for (a) $K_1\to\pi^+\pi^-$, (b) $K_1\to\pi^0\pi^0$, and (c) $K^+\to\pi^+\pi^0$. (Solid circles are strong vertices, and solid squares are weak vertices.)

$$C_8^{(1/2)}+C_{27}^{(1/2)}+C_{27}^{(3/2)}=4.47\ ,$$
$$C_8^{(1/2)}+C_{27}^{(1/2)}-2C_{27}^{(3/2)}=4.21\ .$$

This inconsistency comes from our neglecting the phase shift in the final pions. The right relations are

$$|C_8^{(1/2)}+C_{27}^{(1/2)}+C_{27}^{(3/2)}e^{i(\delta_2-\delta_0)}|=4.47\ ,$$
$$|C_8^{(1/2)}+C_{27}^{(1/2)}-2C_{27}^{(8/2)}e^{i(\delta_2-\delta_0)}|=4.21\ .$$

Here, we assumed that the final-state interactions of pions change the phases, but not the modulus of amplitudes. From these two equations with $C_{27}^{(3/2)}=0.14$, we get

$$C_8^{(1/2)}+C_{27}^{(1/2)}=4.38,\quad C_{27}^{(3/2)}=0.14,\quad \delta_0-\delta_2=53.3^\circ\ . \tag{31}$$

From the phase-shift analysis on the $\pi\pi$ scattering experiments [39], we have $\delta_0-\delta_2=(53\pm5)^\circ$, which agrees with the determination Eq. (31). The other solution $\delta_0-\delta_2=-53.3^\circ$ (mod 360°) is excluded by the above data. If we chose the opposite sign for $C_8^{(1/2)}+C_{27}^{(1/2)}$, we would get the wrong phase shift, $\delta_0-\delta_2$ lying between 90° and 270°.

From $C_{27}^{(3/2)}=5C_{27}^{(1/2)}$, we have

$$C_8^{(1/2)}=4.35,\quad C_{27}^{(1/2)}=0.03\ .$$

This completes our discussion of the basic setup for studying nonleptonic decays of kaons.

IV. $K\to\pi l^+l^-$

In this section, we study $K\to\pi l^+l^-$ decays which are suppressed as a consequence of the flavor-changing neutral current [40]. Among various modes, only $K^+\to\pi^+e^+e^-$ has been seen, with branching ratio $(2.7\pm0.5)\times10^{-7}$ [41]. $K\to\pi l^+l^-$ modes were discussed in great detail in the context of chiral perturbation theory [42], and the decay width for $K^+\to\pi^+e^+e^-$ was used to fix a parameter appearing in the $O(p^4)$ weak Lagrangian. Then, the spectra of $K^+\to\pi^+e^+e^-$ and the decay modes $K^+\to\pi^+\mu^+\mu^-$, $K_S\to\pi^0e^+e^-$, $K_S\to\pi^0\mu^+\mu^-$ were analyzed. Therefore, $K^+\to\pi^+e^+e^-$ is an important process in ChPT, because it is used as an input to fix a parameter which is not constrained by chiral symmetry alone. In our case, the short-distance contributions to $K\to\pi l^+l^-$ from γ,Z^0-exchange penguin diagrams and the W-exchange box diagram generate two new operators [11,12]:

$$Q_{7V}=\frac{e^2}{4\pi}(\bar{s}d)_{V-A}(\bar{l}l)_V\ ,$$
$$Q_{7A}=\frac{e^2}{4\pi}(\bar{s}d)_{V-A}(\bar{l}l)_A\ , \tag{32}$$

with their Hermitian conjugate. In terms of chiral fields, they generate a new effective weak Lagrangian of the form

$$\frac{e^2}{4\pi}[(j_{L\mu})_{23}+(j_{L\mu})_{32}][c_{7V}(\bar{l}l)_V+c_{7A}(\bar{l}l)_A]\ .$$

The imaginary parts of the Wilson coefficients of Q_{7V} and Q_{7A} are reliably calculated in the standard model with leading logarithmic perturbative QCD corrections included. They contribute to direct CP violation from the decay amplitude in $K\to\pi l^+l^-$. On the contrary, the real parts of the Wilson coefficients of Q_{7V} and Q_{7A}, which we are interested in here, are sensitive to the long-distance contribution, and the main contribution comes from the momentum scale below the charm-quark mass, where the leading-logarithmic perturbative QCD is not that reliable. Therefore, it is dangerous to use the real parts of c_{7V} and c_{7A} obtained in the quark level calculations. In the following, we will assume that the contribution of Q_{7A} is negligible compared to other contributions, i.e., only the electromagnetic penguin diagram is considered among three kinds of the short distance contributions. We factor out some trivial factors such as G_F, $e^2/4\pi$, and so on from c_{7V}, defining a new parameter C_7 [see Eq. (37)]. Then, we fix C_7 from the best fit to $B(K^+\to\pi^+e^+e^-)$, and predict other processes such as $K_L\to\pi^0\mu^+\mu^-$, $K_S\to\pi^0e^+e^-$, etc. We have a twofold ambiguity for C_7 and for the predictions, just as ChPT does. For the parameter δ_p, we set $\delta_p=0$ in this section. This choice of parameter will be justified in Sec. VI, and we can absorb the change in δ_p into the change in C_7. The answer will not change very much.

A. $K^+\to\pi^+e^+e^-$ and $K^+\to\pi^+\mu^+\mu^-$

The Feynman diagrams for $K^+\to\pi^+l^+l^-$ are shown in Fig. 4. The general structure of the amplitude for $K^+\to\pi^+\gamma^*$ is

$$\mathcal{M}_\mu(K^+\to\pi^+\gamma^*)=f_1(s)(P_K+p_\pi)_\mu+f_2(s)q_\mu\ ,$$

with $q=P_K-p_\pi$ and $s=q^2$. Current conservation requires $f_1(0)=0$. As long as the operator Q_{7A} is neglected, the q_μ-dependent part does not contribute to $K^+\to\pi^+e^+e^-$. Therefore, we will ignore $f_2(s)$ in the following. In Fig. 4, it looks like double counting of the first graph in (a) and the first graph in (b). However, those two are generated by different left-handed currents, the former by $j_L^A\times j_L^A$ in Eq. (17), and the latter by $j_L^A\times j_L^B$. Also, note that diagrams in (a) and diagrams in (b) are separately gauge invariant. If we omitted the first graph from (a) or (b), gauge invariance would be spoiled. The last graph in Fig. 4(c) is generated by the operator Q_{7V}.

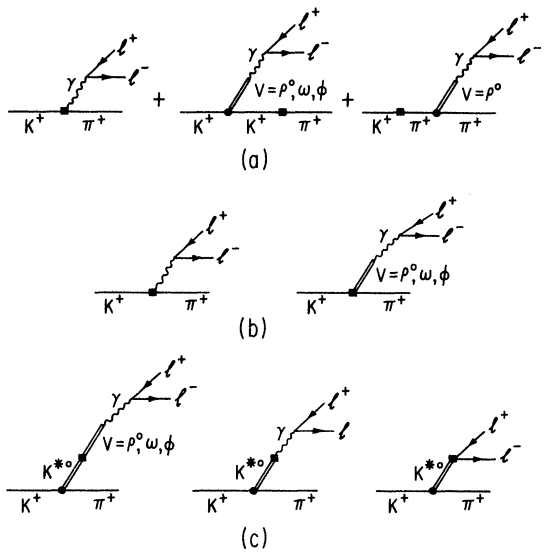

FIG. 4. Feynman diagrams for $K^+\to\pi^+l^+l^-$. (a), (b), and (c) refer to F_a, F_b, F_c defined in Eqs. (35)–(37). (Solid circles are strong vertices, and solid squares are weak vertices.)

Evaluation of the Feynman diagrams shown in Fig. 4 leads to the following expressions (each subscript denotes the Feynman diagrams in Fig. 4):

$$\mathcal{M}_\mu(K^+\to\pi^+\gamma^*)=\frac{C_8^{(1/2)}+C_{27}^{(1/2)}+C_{27}^{(3/2)}}{2\sqrt{2}}G_Ff_\pi^2e(P_K+p_\pi)_\mu F(s)\ , \tag{33}$$

$$F(s)=F_a(s)+F_b(s)+F_c(s)\ , \tag{34}$$

$$F_a(s)=1-\frac{m_K^2}{m_K^2-m_\pi^2}f_\rho(s)-\frac{m_\pi^2}{m_\pi^2-m_K^2}\left[\tfrac{1}{2}f_\rho(s)+\tfrac{1}{6}f_\omega(s)+\tfrac{1}{3}f_\phi(s)\right]\ , \tag{35}$$

$$F_b(s)=-\left[2-\tfrac{3}{2}f_\rho(s)-\tfrac{1}{6}f_\omega(s)-\tfrac{1}{3}f_\phi(s)\right]\ , \tag{36}$$

$$F_c(s)=-\frac{f_{K^*}(s)}{C_8^{(1/2)}+C_{27}^{(1/2)}+C_{27}^{(3/2)}}\left[C_8^{(1/2)}\left[f_\rho(s)-\tfrac{1}{3}f_\omega(s)+\tfrac{2}{3}f_\phi(s)-\tfrac{4}{3}+\tfrac{2}{3}\delta_p(f_\omega(s)-f_\phi(s))\right]\right.$$
$$\left.+C_{27}^{(1/2)}\left[2+f_\rho(s)-f_\omega(s)-2f_\phi(s)\right]+2C_{27}^{(3/2)}\left[1-f_\rho(s)\right]+C_7\frac{s}{m_K^2}\right]\ , \tag{37}$$

where

$$f_V(s)=\frac{m_V^2}{m_V^2-s}\ .$$

Note that each of F_a, F_b, and F_c is gauge invariant by itself. If the vector mesons were neglected (which corresponds to $a=0$), we would get $F=0$ at the tree level, since $F_b=F_c=0$ if $a=0$. Also, $F_a(0)=0$ if the kaon and

the pion are on the mass shell, which is a consequence of gauge invariance and chiral symmetry as noted in Ref. [42]. The form factors arise from the chiral loops ($\pi\pi$, KK, and $K\pi$ loops) in ChPT. In our approach, we get the form factors immediately by vector meson dominance. We set $\delta_p=0$. The new parameter C_7 in $F_c(s)$ is the coefficient of the chiral representation of the operator Q_{7V} defined in Eq. (32).

The invariant amplitude for $K^+\to\pi^+e^+e^-$ becomes

$$\mathcal{M}(K^+\to\pi^+e^+e^-)=\frac{(C_8^{(1/2)}+C_{27}^{(1/2)}+C_{27}^{(3/2)})G_F f_\pi^2 e^2}{2\sqrt{2}} \times\frac{F(s)}{s}\bar{u}(k)(P_K+p_\pi)_\mu\gamma^\mu v(k') , \tag{38}$$

and the decay rate is given by

$$\Gamma(K^+\to\pi^+e^+e^-) =\Gamma_0\int_{4r_l^2}^{(1-r_\pi)^2}dz\,\lambda^{3/2}(1,z,r_\pi^2)\left[1-\frac{4r_l^2}{z}\right]^{1/2} \times\left[1+\frac{2r_l^2}{z}\right]\left|\frac{1}{z}F(z)\right|^2 , \tag{39}$$

where $\lambda(a,b,c)=a^2+b^2+c^2-2(ab+bc+ca)$, $z=q^2/m_K^2$, $r_\pi^2=m_\pi^2/m_K^2$, $r_l^2=m_l^2/m_K^2$, and

$$\Gamma_0=\left[\frac{(C_8^{(1/2)}+C_{27}^{(1/2)}+C_{27}^{(3/2)})G_F f_\pi^2\alpha}{2\sqrt{2}}\right]^2\frac{m_K}{12\pi} =1.83\times10^{-20}\ \text{GeV} .$$

Using the above amplitude and assuming the $SU(3)_f$-symmetric relation, $C_{27}^{(3/2)}=5C_{27}^{(1/2)}$, we get the branching ratio [for $\tau(K^+)=1.24\times10^{-8}$ sec]

$$B(K^+\to\pi^+e^+e^-)=2.1\times10^{-7}$$

for $C_7=0$. This is to be compared with the experimental data [41]

$$B(K^+\to\pi^+e^+e^-)_{\text{expt}}=(2.7\pm0.5)\times10^{-7} .$$

The agreement is quite good, considering that we completely neglected the short-distance contribution by choosing $C_7=0$. However, the effective-mass spectrum of the e^+e^- pair for $C_7=0$ is very different from the phase-space spectrum at low m_{ee}^2. Since the branching ratio was obtained assuming that the spectrum obeys the phase spectrum, we should be rather careful. In fact, a cut with $m_{ee}>140$ MeV (i.e., $s>0.08m_{K^+}^2$) was applied in the experiment, to reject background events from $K_{2\pi}$ Dalitz decay with one soft photon unobserved. Their result with the cut is

$$B(K^+\to\pi^+e^+e^-)_{\text{cut}}=(1.5\pm0.3)\times10^{-7} .$$

If we relax the condition $C_7=0$ and fix C_7 from the best fit to $B(K^+\to\pi^+e^+e^-)_{\text{cut}}$, we have a twofold ambiguity in C_7:

$$C_7=-0.01^{+0.03}_{-0.04}\ \text{ or }\ -0.61^{+0.03}_{-0.04} , \tag{40}$$

We note that the case $C_7=0$ is close to the first solution, and may be regarded as the same within the experimental error and the intrinsic uncertainties in the chiral-Lagrangian approach. This is consistent with zero, and implies that the short-distance contribution of the electromagnetic penguin diagram (Q_{7V}) is not that important in $K^+\to\pi^+e^+e^-$. The other solution $C_7=-0.61$ would imply that the operator Q_{7V} is as important as other operators, O_{1-6} defined in Sec. III (b). For these two values of C_7,

$$(B(K^+\to\pi^+e^+e^-) =\begin{cases}(1.9^{+0.4}_{-0.5})\times10^{-7} & \text{for } C_7=-0.01^{+0.03}_{-0.04} ,\\ (2.9^{+0.6}_{-0.6})\times10^{-7} & \text{for } C_7=-0.61^{+0.03}_{-0.04} .\end{cases}$$

The difference in the branching ratio is the result of difference in the spectra at low m_{ee}. For small s,

$$F(s)\approx(-1.01+1.85-0.96-0.53C_7)\frac{s}{m_\rho^2} =-(0.12+0.53C_7)\frac{s}{m_\rho^2} ,$$

where the first, the second, and the last two terms correspond to Figs. 4(a), 4(b), and 4(c), respectively. We note that there is a destructive interference between the first term (the charge radius term) and the second term, and the result is quite small for $C_7=0$. This is why we observe rather different branching ratios and spectra for different C_7's. In Fig. 5, we show a plot of $B(K^+\to\pi^+e^+e^-)$ with and without the cut as functions of C_7. Also, the fact that $F(s)$ is small for small s renders $F(s)$ sensitive to $C_{27}G_1$'s in spite of its smallness. If we neglect C_{27}'s,

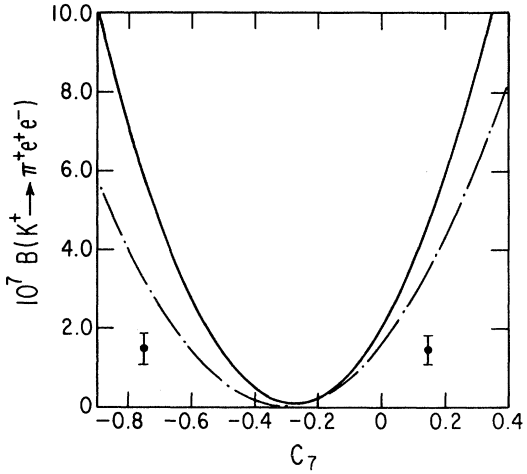

FIG. 5. Dependence of $B(K^+\to\pi^+e^+e^-)$ on C_7: dash-dotted line for $B(K^+\to\pi^+e^+e^-)_{\text{cut}}$, solid line for $B(K^+\to\pi^+e^+e^-)$; with the measured $B(K^+\to\pi^+e^+e^-)_{\text{cut}}$.

TABLE II. Branching ratios for $K\to\pi l^+l^-$ in case C_7 is fixed from the best fit to $K^+\to\pi^+e^+e^-$ with $m_{ee}\geq 140$ MeV; for $K_L\to\pi l^+l^-$, the quoted branching ratios are for indirect CP violation as discussed in the text. The experimental data are taken from Ref. [38], except for $K_L\to\pi^0e^+e^-$, the data of which are taken from Refs. [42] and [43] (in the parentheses).

C_7	$-0.61^{+0.03}_{-0.04}$	$-0.01^{+0.03}_{-0.04}$	Expt. data
$K^+\to\pi^+e^+e^-$ (10^{-7})	$2.9^{+0.6}_{-0.6}$	$1.9^{+0.4}_{-0.5}$	2.6 ± 0.5
$K^+\to\pi^+\mu^+\mu^-$ (10^{-8})	$3.5^{+0.8}_{-1.0}$	$7.0^{+1.2}_{-1.5}$	$<2.3\times10^{-6}$
$K_S\to\pi^0e^+e^-$ (10^{-8})	$4.5^{+0.2}_{-0.2}$	$8.7^{+0.3}_{-0.3}$	$<4.5\times10^{-5}$
$K_S\to\pi^0\mu^+\mu^-$ (10^{-8})	$1.23^{+0.06}_{-0.04}$	$2.29^{+0.06}_{-0.08}$	
$K_L\to\pi^0e^+e^-$ (10^{-11})	$14.0^{+0.6}_{-0.6}$	$27.0^{+0.9}_{-0.9}$	$<5.5(7.5)\times10^{-9}$
$K_L\to\pi^0\mu^+\mu^-$ (10^{-11})	$3.81^{+0.19}_{-0.12}$	$7.10^{+0.19}_{-0.25}$	$<1.2\times10^{-6}$

$$F(s)\approx-(0.18+0.53C_7)\frac{s}{m_\rho^2}\ ,$$

and the branching ratio for $K^+\to\pi^+e^+e^-$ (with the cut) would be 3.6×10^{-7} when $C_7=0$, which is larger than twice the experimental value. On the while, it becomes 0.4×10^{-7} when $C_7=-0.61$. This clearly shows that the $\Delta I=\frac{1}{2}$ rule does not mean that C_{27}'s are always negligible. For $K^+\to\pi^+\mu^+\mu^-$, we find that the branching ratio is predicted to be about (3.5 or 7.0)$\times10^{-8}$, which is well below the present experimental upper limit, 2.3×10^{-6}. See Table II for detail. In the limit of $SU(3)_f$ symmetry (equal vector meson masses), we get $C_7=-0.32$, or -0.88. However, the branching ratios remain essentially the same.

The spectra for $K^+\to\pi^+e^+e^-$ and $K^+\to\pi^+\mu^+\mu^-$ are shown in Fig. 6. As mentioned above, our spectrum of $K^+\to\pi^+e^+e^-$ for $C_7=-0.01$ is very different from the phase-space spectrum and the spectrum for $C_7=-0.61$ in the low-invariant-mass region. The case $C_7=-0.01$ is in sharp contrast to the ChPT calculation which is fairly close to the phase-space spectrum. Above this cut, all the spectra are more or less the same, and we cannot distinguish two models from the spectrum measurement with the cut $m_{ee}\geq140$ MeV. Therefore, the spectrum measurement of $K^+\to\pi^+e^+e^-$ at low m_{ee} can

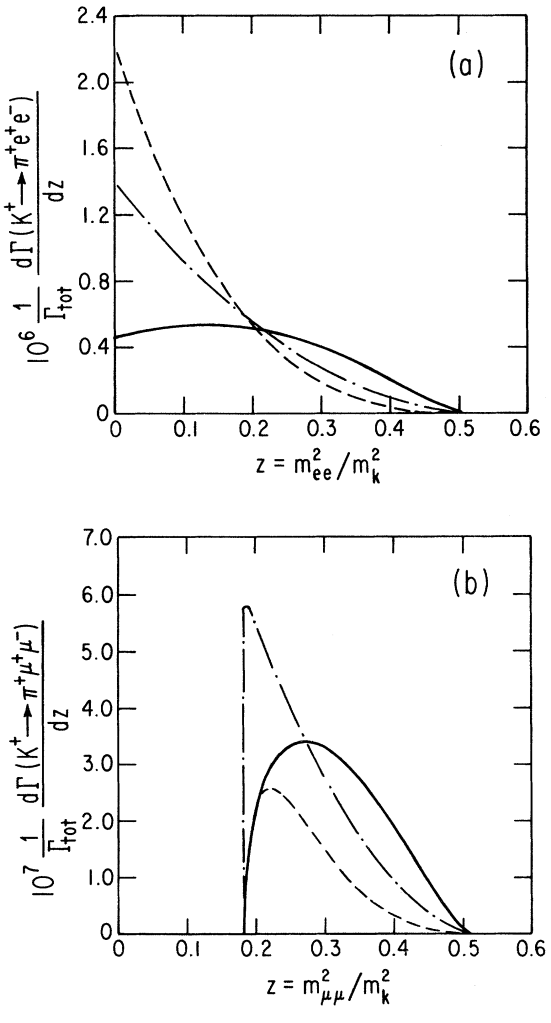

FIG. 6. Dilepton spectra in (a) $K^+\to\pi^+e^+e^-$ and (b) $K^+\to\pi^+\mu^+\mu^-$. (Solid line for $C_7=-0.01$, dashed line for $C_7=-0.61$, and dash-dotted line for the phase-space spectrum.)

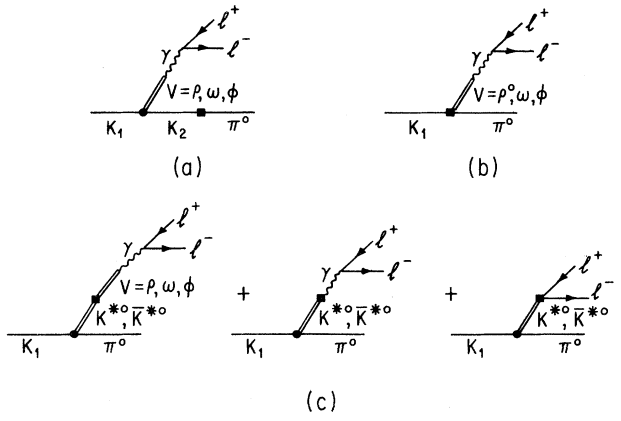

FIG. 7. Feynman diagrams for $K_1\to\pi^0l^+l^-$. (a), (b), and (c) refer to F_a, F_b, F_c defined in Eqs. (43)–(45). (Solid circles are strong vertices, and solid squares are weak vertices.)

fix the twofold ambiguity in C_7. If $C_7=-0.01$ is excluded by experimental data, then we may not ignore c_{7A} any more, and we need data on $K^+\to\pi^+\mu^+\mu^-$ to fix c_{7A}. For the moment, we will content ourselves with $c_{7A}=0$.

B. $K_S\to\pi^0e^+e^-$, $K_S\to\pi^0\mu^+\mu^-$, and $K_L\to\pi^0e^+e^-$

Now, we turn to $K_1\to\pi^0l^+l^-$. The relevant Feynman diagrams are shown in Fig. 7, and we get

$$\mathcal{M}_\mu(K_1\to\pi^0\gamma^*)=\frac{C_8^{(1/2)}+C_{27}^{(1/2)}-2C_{27}^{(3/2)}}{2\sqrt{2}}G_F f_\pi^2 e(P_K+p_\pi)_\mu F(s)\ , \tag{41}$$

$$F(s)=F_a(s)+F_b(s)+F_c(s)\ , \tag{42}$$

$$F_a(s)=\frac{2m_\pi^2}{m_K^2-m_\pi^2}\left[\tfrac{1}{4}f_\rho(s)-\tfrac{1}{12}f_\omega(s)-\tfrac{1}{6}f_\phi(s)\right]\ , \tag{43}$$

$$F_b(s)=\left[\tfrac{1}{2}f_\rho(s)-\tfrac{1}{6}f_\omega(s)-\tfrac{1}{3}f_\phi(s)\right]\ , \tag{44}$$

$$F_c(s)=-\frac{f_{K^*}(s)}{C_8^{(1/2)}+C_{27}^{(1/2)}-2C_{27}^{(3/2)}}\left\{C_8^{(1/2)}\left[\tfrac{4}{3}-f_\rho(s)+\tfrac{1}{3}f_\omega(s)-\tfrac{2}{3}f_\phi(s)-\tfrac{2}{3}\delta_p(f_\omega(s)-f_\phi(s))\right]\right.$$
$$\left.-C_{27}^{(1/2)}[2+f_\rho(s)-f_\omega(s)-2f_\phi(s)]-2C_{27}^{(3/2)}]-2C_{27}^{(3/2)}[1-f_\rho(s)]-C_7\frac{s}{m_K^2}\right\}\ . \tag{45}$$

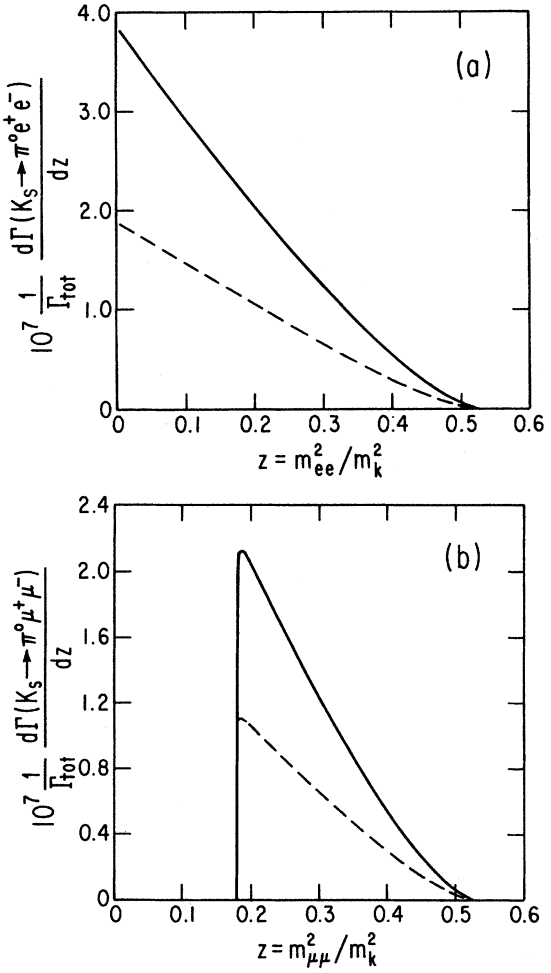

FIG. 8. Dilepton spectra in (a) $K_S\to\pi^0e^+e^-$ and (b) $K_S\to\pi^0\mu^+\mu^-$. (Solid line for $C_7=-0.01$ and dashed line for $C_7=-0.61$.)

For small s, we have

$$F(s)\approx(0.01+0.15+1.06+0.58C_7)\frac{s}{m_\rho^2}$$
$$=(1.22+0.58C_7)\frac{s}{m_\rho^2}\ .$$

We note that Fig. 4(c) gives the most dominant contribution to $K_S\to\pi^0e^+e^-$. The branching ratios for $K_S\to\pi^0e^+e^-$ and $K_S\to\pi^0\mu^+\mu^-$ can be calculated as before, and the results for two values of $C_{27}^{(1/2)}$ are given in Table II. The predicted branching ratios are stable in the $SU(3)_f$ limit (equal vector-meson masses) as before. The spectra are shown in Fig. 8.

Since K_S decays promptly, it is very difficult to measure these decay modes. However, $K_S\to\pi^0e^+e^-$ is still very interesting and important, since it contributes to the indirect CP-violating part of $K_L\to\pi^0e^+e^-$ through mixing. Using the above value for $K_1\to\pi^0e^+e^-$ and the relation

$$B(K_L\to\pi^0e^+e^-)^{\text{indirect}}_{CP\text{ violation}}$$
$$\simeq 3.1\times10^{-3}B(K_S\to\pi^0e^+e^-)\ ,$$

we get

$$B(K_L\to\pi^0e^+e^-)^{\text{indirect}}_{CP\text{ violation}}$$
$$\simeq\begin{cases}(27.0^{+0.9}_{-0.9})\times10^{-11} & \text{for } C_7=-0.01^{+0.03}_{-0.04}\ ,\\ (14.0^{+0.6}_{-0.6})\times10^{-11} & \text{for } C_7=-0.61^{+0.03}_{-0.04}\ .\end{cases} \tag{46}$$

This is still well below the recent bounds from BNL [43] and Fermilab [44], whose new upper limits to $B(K_L\to\pi^0e^+e^0)$ are $(5.5$ and $7.5)\times10^{-9}$, respectively. However, our predictions are substantially larger than ChPT predictions, 1.5×10^{-11} or 1.5×10^{-12}. If our approach is a reasonable scheme for $K\to\pi l^+l^-$, it would be less probable to observe direct CP violation in

$K_L \to \pi^0 e^+ e^-$. This is bad news, since we then have to look for rarer decays such as $K \to \pi \nu \bar{\nu}$ to study direct CP violation in the standard model [45].

C. Discussions

In ChPT, only the $\Delta I = \frac{1}{2}$, $(8_L, 1)$ piece of the weak Lagrangian was considered [42]. If we assume this with $C_7 = 0$, we get $B(K^+ \to \pi^+ e^+ e^-)_{\rm cut} = 3.6 \times 10^{-7}$, which is too large compared with the measured value, $(1.5 \pm 0.3) \times 10^{-7}$. In our approach, we could get a reasonably correct result only when we included the $\Delta I = \frac{1}{2}$ and $\frac{3}{2}$ pieces arising from the $(27_L, 1_R)$ weak Lagrangian. In ChPT, there was a twofold ambiguity as a result of our lack of knowledge of a coefficient in the $O(p^4)$ weak chiral Lagrangian. In our approach, we fix C_7 using the data on $K^+ \to \pi^+ e^+ e^-$, and have a twofold ambiguity for C_7 which will be eventually resolved by measuring the branching ratio of $K^+ \to \pi^+ \mu^+ \mu^-$ and/or the spectrum measurement at low m_{ee} if possible. For $C_7 = -0.61$, the short-distance contribution is not negligible, and Q_{7A} may be as important as Q_{7V}. In this case, both f_1 and f_2 in Eq. (33) can contribute to $K \to \pi l^+ l^-$. For $l = e$, we can still neglect $f_2(s)$ and terms proportional to m_e^2, and we need to add $|C_{7A} f_K^2{}^*(z)|^2$ to $|F(z)/|z|^2$ in Eq. (39). For $l = \mu$, Eq. (40) gets more complicated since we cannot neglect $f_2(s)$ any more. Therefore, the predictions for $C_7 = -0.61$ should be considered with these possible corrections from Q_{7A}.

In the calculations based on the effective Hamiltonian expressed in terms of quark fields [9–12], we have two crucial points: calculation of the Wilson coefficients and evaluation of the matrix elements of the four-quark operators between two states, $|K\rangle$ and $|\pi l^+ l^-\rangle$. The electromagnetic penguin diagram gives only a quarter of the decay rate for $K^+ \to \pi^+ e^+ e^-$, and it is important to calculate the contributions from other operators up to $O(e^2)$. However, the QCD corrections to the Wilson coefficients of those operators are very large, and even change their signs. Therefore, we should be cautious in working in this framework as emphasized in Refs. [10–12]. Also, it is usually assumed that the $sd\gamma$ electromagnetic penguin diagram is the largest contribution to $K_L \to \pi^0 e^+ e^-$, for example. However, the analysis done in Refs. [11] and [46] shows that the $sd\gamma$ electromagnetic penguin diagram alone predicts too small decay rates for weak radiative decays of kaons and hyperons, and nonelectromagnetic penguin contributions are also important. Therefore, it is dangerous to consider only the $sd\gamma$ contribution in discussing $K \to \pi l^+ l^-$. The importance of another operator, $sd\gamma g$ where g is the gluon, in weak radiative decays of hyperons was considered in Ref. [47], but there are still uncertainties coming from evaluation of the matrix element of such an operator. To evaluate the matrix elements of the four-quark operators, we need to know the relations between quark fields and meson fields. It is usually done by comparing the left-handed current from the effective Lagrangian and the left-handed current from the standard model. However, the Wilson coefficients in the quark picture are renormalization-scale dependence, and it is not clear how to identify the scale in the quark picture with some scale in the meson picture. This is important to guarantee that the S-matrix elements be independent of the renormalization scale. Thus, it is not that simple to get quantitative results on nonleptonic kaon decays in the quark picture.

V. $K_L \to \gamma\gamma$ AND $K_L \to \gamma l^+ l^-$

In this section, we discuss $K_L \to \gamma\gamma$, $K_L \to \gamma e^+ e^-$, and $K_L \to \gamma \mu^+ \mu^-$. In these processes, the pseudoscalar poles give the main contributions, though the form factor of the off-mass-shell photon is governed by vector meson form factors. In calculating these decay modes, there are some uncertainties. First of all, we need to understand the effect of the $SU(3)_f$ singlet η_0, its decay constant, its mixing with the $SU(3)_f$-octet isoscalar η_8, and the relations among $a(K_2\pi^0)$, $a(K_2\eta_8)$ and $a(K_2\eta_0)$. For each quantity, there is some uncertainty. Therefore, we start with general analyses without assuming nonet symmetry. Then, we will do the numerical analysis with some specific assumptions. It will be found that the deviation of the form factor of the virtual photon in $K_L \to \gamma l^+ l^-$ from the ρ form factor has some correlation with the spectrum of the low-energy photon pair in $K_L \to \pi^0 \gamma\gamma$.

A. $K_L \to \gamma\gamma$

To begin with, we define a form factor $F_{P\gamma\gamma}(q^2)$ by

$$\mathcal{M}(P \to \gamma(q,\epsilon)\gamma(q',\epsilon')) = \epsilon_{\mu\nu\alpha\beta} q^\mu \epsilon^\nu q'^\alpha \epsilon'^\beta F_{P\gamma\gamma}(q^2) , \quad (47)$$

where we set $q'^2 = 0$ while q^2 is arbitrary. Here P denotes a CP-odd pseudoscalar meson such as π^0, η, η', etc. For $K_L \to \gamma\gamma$, the branching ratio is measured [37] to be $B(K_L \to \gamma\gamma) = (5.70 \pm 0.27) \times 10^{-4}$. From

$$\Gamma(P \to \gamma\gamma) = \frac{m_P^2}{64\pi} |F_{P\gamma\gamma}(0)|^2 ,$$

we can determine $|F_{K_2\gamma\gamma}(0)|$:

$$|F_{K_2\gamma\gamma}(0)| = (3.43 \pm 0.08) \times 10^{-12}\ \text{MeV}^{-1} . \quad (48)$$

In our model, only the pseudoscalar pole diagrams contribute to $K_L \to \gamma\gamma$ (see Fig. 9):

$$F_{K_2\gamma\gamma}(0) = -\frac{a(K_2\pi^0)}{m_K^2} \left[\frac{F_{\pi\gamma\gamma}(0)}{1-r_\pi^2} + \frac{F_{\eta\gamma\gamma}(0)}{1-r_\eta^2}\zeta + \frac{F_{\eta'\gamma\gamma}(0)}{1-r_{\eta'}^2}\zeta' \right] , \quad (49)$$

where $\zeta = a(K_2\eta)/a(K_2\pi^0)$, $\zeta' = a(K_2\eta')/a(K_2\pi^0)$, and $r_P^2 = m_P^2/m_{K_L}^2$. In the above equation, $F_{\eta\gamma\gamma}(0)$ and $F_{\eta'\gamma\gamma}(0)$ depend on the mixing angle between η_8 and η_0 and their decay constants. However, we can avoid referring to those quantities by directly using the measurements [48] of $\eta, \eta' \to \gamma\gamma$. From

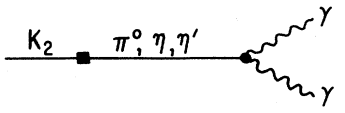

FIG. 9. Feynman diagram for $K_L \to \gamma\gamma$.

$$\Gamma(\eta \to \gamma\gamma) = (0.51 \pm 0.02 \pm 0.04)\ \text{keV} ,$$

$$\Gamma(\eta' \to \gamma\gamma) = (4.7 \pm 0.5 \pm 0.5)\ \text{keV} ,$$

we easily find that [49]

$$F_{\eta\gamma\gamma}(0) = (2.49 \pm 0.10) \times 10^{-5}\ \text{MeV}^{-1} ,$$

$$F_{\eta'\gamma\gamma}(0) = (3.28 \pm 0.24) \times 10^{-5}\ \text{MeV}^{-1} .$$

For $a(K_2\pi^0)$, there are two values in the literature: (i) one is the naive value obtained from the chiral Lagrangian, and (ii) the other is gotten from $K_S \to 2\pi$ with final interactions taken into account [50]. For the moment, we parametrize $a(K_2\pi^0)$ by

$$\frac{a(K_2\pi^0)}{m_K^2} = -\wp \frac{2G_F f_\pi^2}{\sqrt{2}} ,$$

or

$$a(K_2\pi^0) = -(3.55\wp) \times 10^{-2}\ \text{MeV}^{-2}\ \text{MeV}^{-2} .$$

Case (i) corresponds to $\wp = 1.00$, and the case (ii) to $\wp = 0.82$. In terms of the three parameters ζ, ζ', and $\wp$, Eqs. (48) and (49) reduce to

$$\wp(1 - 4.32\zeta - 0.45\zeta') = \pm 0.89 . \tag{50}$$

This is one relation among ζ, ζ', and $\wp$ obtained from the data on $K_L \to \gamma\gamma$.

In passing, we shortly discuss $K_S \to \gamma\gamma$. Both ChPT [51] and the pion rescattering model [52] predict $B(K_S \to \gamma\gamma) = 2.0 \times 10^{-6}$, compared to the measured value of $(2.4 \pm 1.2) \times 10^{-6}$ [53]. For this decay mode, the main contribution comes from the pion loop, and there is no kaon loop contribution in ChPT. Therefore, it occurs through $K_S \to \pi^+\pi^- \to \gamma\gamma$. In our model, vector meson contribution modifies $\pi^+\pi^- \to \gamma\gamma$. But it is higher order and has been shown to be negligible in Ref. [5].

B. $K_L \to \gamma l^+ l^-$

Now, we turn to $K_L \to \gamma l^+ l^-$. First, we normalize $\Gamma(K_L \to \gamma l^+ l^-)$ to $\Gamma(K_L \to \gamma\gamma)$ for convenience. If we renormalize $F_{P\gamma\gamma}(q^2)$ to $F_{P\gamma\gamma}(0)$ by defining

$$\tilde{F}_{P\gamma\gamma}(q^2) = \frac{F_{P\gamma\gamma}(q^2)}{F_{P\gamma\gamma}(0)} ,$$

so that $\tilde{F}_{P\gamma\gamma}(0) = 1$, we can easily derive that

$$\frac{1}{\Gamma(K_L \to \gamma\gamma)} \frac{d\Gamma(K_L \to \gamma l^+ l^-)}{ds} = \frac{2\alpha}{3\pi} \frac{1}{s} \left[1 - \frac{s}{m_K^2}\right]^3 \left[1 + \frac{2m_l^2}{s}\right] \times \left[1 - \frac{4m_l^2}{s}\right]^{1/2} |\tilde{F}_{K_2\gamma\gamma}(s)|^2 ,$$

with $s = q^2$.

The Feynman diagrams for $K_L \to \gamma l^+ l^-$ are shown in Fig. 10. First of all, Fig. 10(a) is very similar to Fig. 9 for $K_L \to \gamma\gamma$, and was considered in Ref. [54]. The off-shell photon can be dominated by vector mesons, ρ, ω, and ϕ. Its contribution to $\tilde{F}_{K_2\gamma\gamma}(s)$ is

$$\tilde{F}^{(a)}_{K_2\gamma\gamma}(s) = \frac{\tilde{F}_{\pi\gamma\gamma}(s) - 4.32\zeta\tilde{F}_{\eta\gamma\gamma}(s) - 0.45\zeta'\tilde{F}_{\eta'\gamma\gamma}(s)}{1 - 4.32\zeta - 0.45\zeta'} , \tag{51}$$

where

$$\tilde{F}_{\pi\gamma\gamma}(s) = f_\rho(s) ,$$

$$\tilde{F}_{\eta\gamma\gamma}(s) = \frac{\frac{10}{3}X_{\eta\rho}f_\rho(s) - \frac{2}{3}Y_{\eta\phi}f_\phi(s)}{\frac{10}{3}X_{\eta\rho} - \frac{2}{3}Y_{\eta\phi}} ,$$

$$\tilde{F}_{\eta'\gamma\gamma}(s) = \frac{\frac{10}{3}X_{\eta'\rho}f_\rho(s) - \frac{2}{3}Y_{\eta'\phi}f_\phi(s)}{\frac{10}{3}X_{\eta'\rho} - \frac{2}{3}Y_{\eta'\phi}} .$$

We neglected the mass difference between ρ and ω, and set $f_\rho(s) = f_\omega(s)$. Here, $X_{\eta\rho}$, $X_{\eta'\rho}$, $Y_{\eta\phi}$, and $Y_{\eta'\phi}$ are given by

$$X_{\eta\rho} = \left[\frac{f_\pi}{f_8}\frac{\cos\theta_P}{\sqrt{3}} - \frac{f_\pi}{f_0}\left[\frac{2}{3}\right]^{1/2}\sin\theta_P\right] = 0.72 ,$$

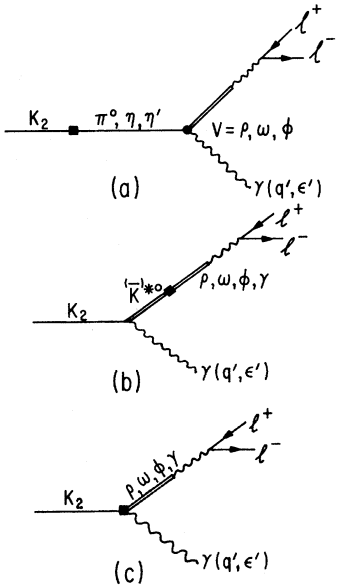

FIG. 10. Feynman diagrams for $K_L \to \gamma l^+ l^-$.

$$X_{\eta'\rho}=\frac{f_\pi}{f_8}\frac{\sin\theta_P}{\sqrt{3}}+\frac{f_\pi}{f_0}\left[\frac{2}{3}\right]^{1/2}\cos\theta_P=0.57\ ,$$
$$Y_{\eta\phi}=\frac{f_\pi}{f_8}\frac{2\cos\theta_P}{\sqrt{3}}+\frac{f_\pi}{f_0}\left[\frac{2}{3}\right]^{1/2}\sin\theta_P=0.60\ , \quad (52)$$
$$Y_{\eta'\phi}=\frac{f_\pi}{f_8}\frac{2\sin\theta_P}{\sqrt{3}}-\frac{f_\pi}{f_0}\left[\frac{2}{3}\right]^{1/2}\cos\theta_P=-1.07\ ,$$

where we used the following values [49] for f_8, f_0, and θ_P:

$$\frac{f_8}{f_\pi}=1.23,\quad \frac{f_0}{f_\pi}=1.04,\quad \theta_P=-20.8^\circ\ .$$

Then, we find that

$$\tilde{F}^{(a)}_{K_2\gamma\gamma}(s)=f_\rho(s)+[f_\rho(s)-f_\phi(s)]\frac{0.12\zeta'-0.86\zeta}{1-4.32\zeta-0.45\zeta'}\ . \quad (53)$$

We note that there is some deviation from the pure ρ form factor in general, unless $0.12\zeta'-0.86\zeta=0$.

The second diagram, Fig. 10(b), was considered in Ref. [55]. The weak vertex with two vector mesons is coming from the left-handed current:

$$j_{L\mu}=-2f_\pi^2(gV_\mu-eQA_\mu)\ .$$

The other vertex, $K^*K_2\gamma$, comes from the anomalous Lagrangian involving $V\pi\gamma$ in Eq. (16). Evaluation of Fig. 10(b) leads to

$$\tilde{F}^{(b)}_{K_2\gamma\gamma}(s)=\frac{(1-r_\pi^2)f_{K^*}(s)}{2\wp(1-4.32\zeta-0.45\zeta')}\times\{C_8^{(1/2)}\tfrac{1}{3}[2-f_\rho(s)-f_\phi(s)-\delta_p(f_\rho(s)-f_\phi(s))]-C_{27}^{(1/2)}[1-f_\phi(s)]-C_{27}^{(3/2)}[1-f_\rho(s)]\}\ . \quad (54)$$

If Fig. 10(a) and 10(b) were all the relevant diagrams to $K_L\to\gamma l^+l^-$, we would get into trouble unless we introduced some arbitrary constant multiplying the vector-meson contribution, $\tilde{F}^{(b)}_{K_2\gamma\gamma}(s)$, to reduce its relative strength compared to $\tilde{F}^{(a)}_{K_2\gamma\gamma}(s)$. This was actually done in Ref. [55]. In our approach, we cannot introduce such an arbitrary constant. The relative strengths and signs among chiral amplitudes and vector meson amplitudes are all fixed from the beginning, since they are all generated from the same Lagrangian.

In our model, this trouble actually does not occur, since there is another diagram, Fig. 10(c), which contains a *weak* $V\pi\gamma$ vertex. The octet piece of this new diagram largely cancels that of Fig. 10(b), as shown below. Let us note that the anomalous left-handed current, Eq. (24), can produce a weak $V\pi\gamma$ vertex when it is combined with a normal current, $j_{L\mu}=-f_\pi D_\mu\pi$. These new weak $V\pi\gamma$ vertices take part in $K_L\to\gamma l^+l^-$ and $K_L\to\pi^0\gamma\gamma$, and can be read off from the following Lagrangians:

$$\mathcal{L}^{\Delta I=1/2}_{(8,1)}(V\pi\gamma)=\frac{C_8^{(1/2)}G_F}{6\sqrt{2}}g_{\omega\pi\gamma}\epsilon^{\mu\nu\alpha\beta}\partial_\mu A_\nu\times\left[\sqrt{2}\,\pi^0(K^{*0}_{\alpha\beta}+\bar{K}^{*0}_{\alpha\beta})-2K_2\left[(-\rho^0+\omega)_{\alpha\beta}-\sqrt{2}\,\phi_{\alpha\beta}+\frac{4e}{3g}\partial_\alpha A_\beta\right]\right.$$
$$\left.-2\delta_pK_2\left[(3\rho^0+\omega)_{\alpha\beta}+\sqrt{2}\,\phi_{\alpha\beta}-\frac{4e}{3g}\partial_\alpha A_\beta\right]\right]\ , \quad (55)$$

$$\mathcal{L}^{\Delta I=1/2}_{(27,1)}=\frac{C_{27}^{(1/2)}G_F}{6\sqrt{2}}g_{\omega\pi\gamma}\epsilon^{\mu\nu\alpha\beta}\partial_\mu A_\nu\left[-\sqrt{2}\pi^0(K^{*0}_{\alpha\beta}+\bar{K}^{*0}_{\alpha\beta})+2K_2\left[4\rho^0_{\alpha\beta}-3\sqrt{2}\,\phi_{\alpha\beta}-\frac{2e}{g}\partial_\alpha A_\beta\right]\right]\ , \quad (56)$$

$$\mathcal{L}^{\Delta I=3/2}_{(27,1)}=\frac{C_{27}^{(3/2)}G_F}{6\sqrt{2}}g_{\omega\pi\gamma}\epsilon^{\mu\nu\alpha\beta}\partial_\mu A_\nu\left[2\sqrt{2}\pi^0(K^{*0}_{\alpha\beta}+\bar{K}^{*0}_{\alpha\beta})+2K_2\left[\rho^0_{\alpha\beta}+3\omega_{\alpha\beta}-\frac{2e}{g}\partial_\alpha A_\beta\right]\right]\ . \quad (57)$$

Here, $V_{\alpha\beta}\equiv\partial_\alpha V_\beta$, and

$$g_{\omega\pi\gamma}=-\frac{30Cieg}{f_\pi}=-\frac{3eg}{8\pi^2f_\pi}\ . \quad (58)$$

From this, we can evaluate Fig. 10(c) and the result is

$$\tilde{F}^{(c)}_{K_2\gamma\gamma}(s)=-\frac{1-r_\pi^2}{2\wp(1-4.32\zeta-0.45\zeta')}\times\{C_8^{(1/2)}\tfrac{1}{3}[2-f_\rho(s)-f_\phi(s)-\delta_p(6-5f_\rho(s)-f_\phi(s))]+C_{27}^{(1/2)}[1-2f_\rho(s)+f_\phi(s)]+C_{27}^{(3/2)}[1-f_\rho(s)]\}\ . \quad (59)$$

By comparing the octet piece of $\tilde{F}^{(b)}_{K_2\gamma\gamma}$ and $\tilde{F}^{(c)}_{K_2\gamma\gamma}$, we find that s/m_ρ^2 terms cancel and the leading term is of order $(s/m_\rho^2)^2$ for small s if $\delta_p=0$. The actual form factor $\tilde{F}_{K_2\gamma\gamma}(s)$ is the sum of three diagrams, Figs. 10(a), 10(b), and 10(c):

$$\tilde{F}_{K_2\gamma\gamma}(s)=\tilde{F}^{(a)}_{K_2\gamma\gamma}(s)+\tilde{F}^{(b)}_{K_2\gamma\gamma}(s)+\tilde{F}^{(c)}_{K_2\gamma\gamma}(s)\ . \tag{60}$$

Only the first form factor contributes to $K_L\to\gamma\gamma$ when $s=q^2=0$, and reduces to 1, which is the case of the previous subsection. The other two vanish at $s=q^2=0$: $\tilde{F}^{(b)}_{K_2\gamma\gamma}(0)=\tilde{F}^{(c)}_{K_2\gamma\gamma}(0)=0$, and do not contribute to $K_L\to\gamma\gamma$.

C. Numerical analysis

Up to now, we have left ζ, ζ' and $\wp$ unspecified. To analyze the data on $K_L\to\gamma\gamma$ and $K_L\to\gamma l^+l^-$, we start by assuming $SU(3)_f$ symmetry, which enables us to write down

$$\frac{a(K_2\eta_8)}{a(K_2\pi^0)}=\frac{1}{\sqrt{3}}\frac{C_8^{(1/2)}-9C_{27}^{(1/2)}}{C_8^{(1/2)}+C_{27}^{(1/2)}-2C_{27}^{(3/2)}}\frac{f_8}{f_\pi}\ .$$

For $a(K_2\eta_0)$, we make the following ansatz:

$$\frac{a(K_2\eta_0)}{a(K_2\pi^0)}=-\left[\frac{2}{3}\right]^{1/2}\frac{C_8^{(1/2)}}{C_8^{(1/2)}+C_{27}^{(1/2)}-2C_{27}^{(3/2)}}\times\frac{f_0}{f_\pi}(2-3\delta_n)\ .$$

Here, we introduced a new parameter, δ_n. If there were no QCD axial anomaly and η_0 were the ninth Nambu-Goldstone boson, we would have $\delta_n=\delta_p$. However, δ_n is different from δ_p in general, and nonet symmetry in the pseudoscalar-nonet sector would be realized when $\delta_n=\delta_p$. Assuming the above equations with δ_n unspecified, we can express ζ and ζ' in terms of δ_n only. Plugging these expressions with $\theta_P=-20.8°$ into Eq. (50) obtained from the data on $K_L\to\gamma\gamma$, we get

$$1-4.32\zeta-0.45\zeta'=1.79-5.29\delta_n=\pm\frac{0.89}{\wp}\ .$$

For $\wp=0.82$, we have two solutions for δ_n:

$$\delta_n=0.13\ \text{ or }\ 0.54\ . \tag{61}$$

For each δ_n, and for various values of δ_p, we can make plots for $|\tilde{F}_{K_2\gamma\gamma}(s)|^2$ with varying δ_p, and then compare with the measured one in $K_L\to\gamma e^+e^-$. Thus, we obtain

$$\delta_p=\begin{cases}-0.3\le\delta_p\le0.4 & \text{for } \delta_n=0.54\ ,\\ -1.9\le\delta_p\le-1.2 & \text{for } \delta_n=0.13\ .\end{cases} \tag{62}$$

These constraints on δ_p are not that tight, although there is little difference in the branching ratios of $K_L\to\gamma e^+e^-$ and $K_L\to\gamma\mu^+\mu^-$. In the next section on $K_L\to\pi^0\gamma\gamma$, we will find that the recent measurement of the two-photon spectrum in the decay mode $K_L\to\pi^0\gamma\gamma$ also provides us with a constraint on δ_p that is stronger than what we got in this section [see Fig. 14(b)]:

$$-0.06\le\delta_p\le0.20\ \text{ for }\ \delta_n=0.54\ . \tag{63}$$

To simplify the following discussions, we will consider only this choice of parameters in the rest of this section. In Fig. 11(a), we give the plot of $|\tilde{F}_{K_2\gamma\gamma}(s)|^2$ for $\delta_p=0.00^{+0.20}_{-0.06}$ and $\delta_n=0.54$. The other case, $\delta_n=0.13$ and $\delta_p=-1.5^{+0.3}_{-0.4}$ is shown in Fig. 11(b). (The $\delta_p=0$ case is also shown for comparison. $\delta_p=0$ is clearly excluded for $\delta_n=0.13$.) However, this case will be excluded in the next section on the grounds that it leads to too large a branching ratio, and the two-photon spectrum at low $m_{\gamma\gamma}$ in the process $K_L\to\pi^0\gamma\gamma$ is enhanced too much in contrast to the recent measurement.

For the above choice of δ_n and δ_p, Eq. (63), we predict

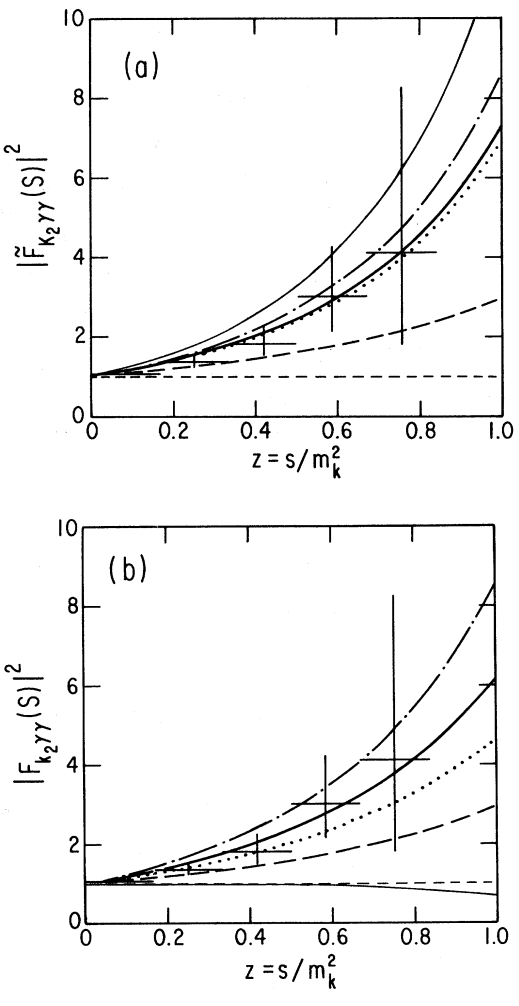

FIG. 11. Plots of $|\tilde{F}_{K_2\gamma\gamma}(s)|^2$. (a) For $\delta_n=0.54$: thick solid line for $\delta_p=0.0$, dotted line for $\delta_p=-0.06$, dash-dotted line for $\delta_p=0.20$, and thin solid line for $\delta_p=0.64$. (b) For $\delta_n=0.13$: Solid line for $\delta_p=-1.5$, dotted line for $\delta_p=-1.2$, dash-dotted line for $\delta_p=-1.9$, and thin solid line for $\delta_p=0$. In (a) and (b), the dashed line is for the pure ρ form factor, and the short-dashed line is for pure QED. The data are taken from Ref. [13].

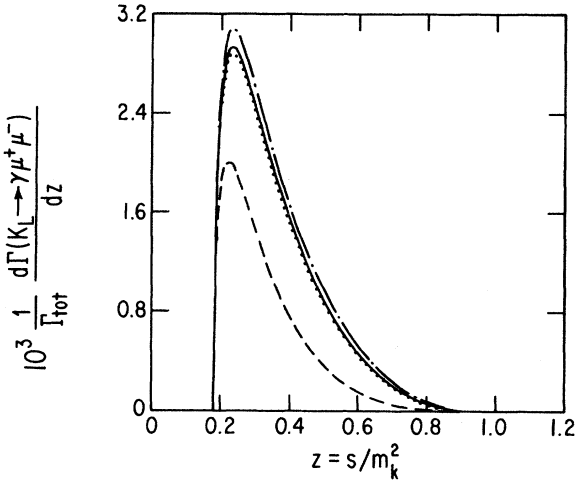

FIG. 12. Dimuon spectrum in $K_L \to \gamma\mu^+\mu^-$ for $\delta_n = 0.54$: Solid line for $\delta_p = 0.0$, dotted line for $\delta_p = -0.06$, dash-dotted line for $\delta_p = 0.20$, and dashed line for the phase-space spectrum.

that

$$\frac{1}{\Gamma(K_L \to \gamma\gamma)} \frac{d\Gamma(K_L \to \gamma e^+ e^-)}{ds} = (1.67^{+0.02}_{-0.01}) \times 10^{-2} \quad (1.58 \times 10^{-2}) ,$$

$$\frac{1}{\Gamma(K_L \to \gamma\gamma)} \frac{d\Gamma(K_L \to \gamma\mu^+\mu^-)}{ds} = (7.45^{+0.54}_{-0.15}) \times 10^{-4} \quad (4.10 \times 10^{-4}) .$$

The rates for the phase-space spectra, $\tilde{F}_{K_2\gamma\gamma}(s) = 1$, are shown in the parentheses. In particular, we have

$$\frac{\Gamma(K_L \to \gamma e^+ e^-)}{\Gamma(K_L \to \gamma\mu^+\mu^-)} \simeq 22.4 \quad (38.5) .$$

For $K_L \to \gamma e^+ e^-$, there is very little difference, and both values are in good agreement with the recent measurements $B(K_L \to \gamma e^+ e^-) = (9.2 \pm 0.5 \pm 0.5) \times 10^{-6}$ [13] and $(9.1 \pm 0.4^{+0.6}_{-0.4}) \times 10^{-6}$ [14]. The spectrum of the Dalitz pair from $K_L \to \gamma e^+ e^-$ is dominated by the $1/s$ factor. For the process $K_L \to \gamma\mu^+\mu^-$, our model predicts that the branching ratio of $K_L \to \gamma\mu^+\mu^-$ is enhanced over the phase-space value by almost a factor of 2. This is in contrast to the ChPT prediction, where the branching ratio is essentially the same as the phase-space value [1]. The present measurement of $B(K_L \to \gamma\mu^+\mu^-) = (2.8 \pm 2.8) \times 10^{-7}$ cannot distinguish our prediction from others. The dimuon spectrum in $K_L \to \gamma\mu^+\mu^-$ is shown in Fig. 12 with the phase-space spectrum.

If one can measure $B(K_L \to \gamma\mu^+\mu^-)$ accurately enough, we get a tighter constraint for δ_p. Or, the precise measurement of $|F_{K_2\gamma\gamma}(s)|^2$ at large s around $m_{K_L}^2$, say, will do the same job. The measurements of $K_L \to \gamma e^+ e^-$ and $K_L \to \gamma\mu^+\mu^-$ are still uncertain, and are to be used to distinguish various models. Understanding these decays more accurately is very important, since they can be backgrounds for rarer decays such as $K_L \to \pi^0 e^+ e^-$ and $K_L \to \pi^0 \mu^+ \mu^-$.

VI. $K_L \to \pi^0\gamma\gamma$ AND ITS CONTRIBUTION TO $K_L \to \pi^0 e^+ e^-$

A. Present status of $K_L \to \pi^0\gamma\gamma$

$K_L \to \pi^0\gamma\gamma$ is an interesting process not only for its own sake, but also for its contribution as a dominant intermediate state to the CP-conserving two-photon-exchange process [1,2] in $K_L \to \pi^0 e^+ e^-$. Since $K_L \to \pi^0 e^+ e^-$ has the potential to display the effect of direct CP violation predicted by the standard model with three families [11,12], it is very important to understand the possible background through $K_L \to \pi^0\gamma\gamma \to \pi^0 e^+ e^-$.

For $K_L \to \pi^0\gamma\gamma$, the main contributions come from the chiral loop [1] or two-pion intermediate state [3], and possibly from vector-meson exchange [4,5]. There is consensus about the first contribution. Both ChPT and the rescattering model predict $B(K_L \to \pi^0\gamma\gamma)$ to be around 7×10^{-7}, and the two-photon spectrum is peaked around $m_{\gamma\gamma} \simeq 300$ MeV, though the peak in the pion rescattering model is located at slightly higher $m_{\gamma\gamma}$ than the peak in ChPT. Since two photons produced through this process have total angular momenta $J = 0$ and m_e is very small, they are not effective in making the $e^+ e^-$ pair as a result of helicity suppression. In fact, the branching ratio of $K_L \to \pi^0 e^+ e^-$ through the exchange of two photons in $J = 0$ is estimated to be around 10^{-14} [1], which is small compared to the branching ratio of $K_L \to \pi^0 e^+ e^-$ with direct CP violation [12] (around 10^{-11}). If the two-photon contribution were indeed so small, we could safely ignore the CP-conserving contribution to $K_L \to \pi^0 e^+ e^-$. However, the exchange of vector mesons produces both $J = 0$ and $J = 2$ photons, and the $J = 2$ photons can produce the $e^+ e^-$ pair without any suppression. The two-photon spectrum with both chiral loop and the vector-meson amplitudes included exhibits enhancement below the pion pair threshold. Unfortunately, there has been no consensus about the importance of the vector-meson contributions despite various attempts.

Recent data [6] reported observation of some signals, but their result is puzzling, rather than resolving the theoretical discrepancies. The spectrum seems to be consistent with the assumption that the vector mesons are not important. Specifically,

$$R = \frac{\Gamma(0 \le m_{\gamma\gamma} \le 100 \text{ MeV}) + \Gamma(170 \text{ MeV} \le m_{\gamma\gamma} \le 240 \text{ MeV})}{\Gamma(0 \le m_{\gamma\gamma} \le 100 \text{ MeV}) + \Gamma(170 \text{ MeV} \le m_{\gamma\gamma})} < 0.12 . \quad (64)$$

The branching ratio for $m_{\gamma\gamma} \geq 280$ MeV is large $[(2.1 \pm 0.6) \times 10^{-6}]$, which is too large compared with the prediction, 7×10^{-7}.

Therefore, it should be worthwhile to study the subject more carefully. In the previous study of the vector-meson contribution to $K_L \to \pi^0 \gamma\gamma$, only one diagram [Fig. 13(a)] was considered [4,5] among many possible diagrams [Figs. 13(a)–13(e)]. In particular, direct emissions of vector meson(s) were ignored without any justification. There has been some suggestion (weak deformation model) by Ecker *et al.* [56] regarding this possibility, which predicts a rather small contribution of the vector mesons to $K_L \to \pi^0 \gamma\gamma$. However, their assumption is highly nontrivial, and it lies beyond the scope of chiral symmetry. One has to await, for example, precise measurement of $K^+ \to \pi^+ \gamma\gamma$ to test their model. In our model, we can study the direct emissions of the vector meson(s) in a systematic way with chiral symmetry respected at every stage. In the rest of this section, we give a detailed analysis of this problem in our framework.

Before we consider the individual diagrams contributing to $K_L \to \pi^0 \gamma\gamma$, we note that the general form of the amplitude for $K_L \to \pi^0 \gamma\gamma$ is given by [1,5]

$$\begin{aligned} &\mathcal{M}(K_L(P) \to \pi^0(p) + \gamma(k,\epsilon)\gamma(k',\epsilon')) \\ &\quad = A(s,t,u)(k\cdot\epsilon' k'\cdot\epsilon - k\cdot k'\epsilon\cdot\epsilon') \\ &\qquad + B(s,t,u)\frac{P\cdot kP\cdot k'}{k\cdot k'}\epsilon\cdot\epsilon' \ . \end{aligned} \tag{65}$$

Then the decay rate is obtained by integrating the following expression over s:

$$\frac{d\Gamma}{ds} = \frac{1/4}{256 m_{K_L}^3 \pi^3} \int_{t_0}^{t_1} dt \left[|As - m_{K_L}^2 B|^2 + \frac{|B|^2}{s^2}(m_{\pi^0}^2 m_{K_L}^2 - tu)^2 \right] , \tag{66}$$

where the limits of the integration are $[s = (k + k')^2]$

$$\begin{aligned} &t_0 \leq t \leq t_1, \quad 0 \leq s \leq (m_{K_L} - m_{\pi^0})^2 \ , \\ &t_{1,0} = \tfrac{1}{2}[\,(m_{K_L}^2 + m_{\pi^0}^2 - s) \\ &\qquad \pm \sqrt{(m_{K_L}^2 + m_{\pi^0}^2 - s)^2 - 4 m_{\pi^0}^2 m_{K_L}^2}\,] \ . \end{aligned}$$

Here, $A = A_{\rm ch} + A_V$ and $B = B_{\rm ch} + B_V$, where $A_{\rm ch}$ and A_V denote the chiral amplitude and vector-meson amplitude, and similarly for $B_{\rm ch}$ and B_V. Note that $d\Gamma/ds$ gives the spectrum of two photons.

We quote the result for $A_{\rm ch}(s,t,u)$ of $O(p^4)$ due to the chiral loop from Ref. [1] without repeating the explicit calculation here:

$$A_{\rm ch}^{\rm loop} = \frac{G_8 \alpha}{\pi} \left[\left(1 - \frac{m_{\pi^+}^2}{s}\right) F\left(\frac{s}{m_{\pi^+}^2}\right) - \left(1 - \frac{m_{K^+}^2}{s} - \frac{m_{\pi^+}^2}{s}\right) F\left(\frac{s}{m_{K^+}^2}\right) \right] , \tag{67}$$

$$B_{\rm ch}^{\rm loop} = 0 \ ,$$

where $G_8 \alpha m_{K_L}^2 / \pi = 5.24 \times 10^{-9}$,

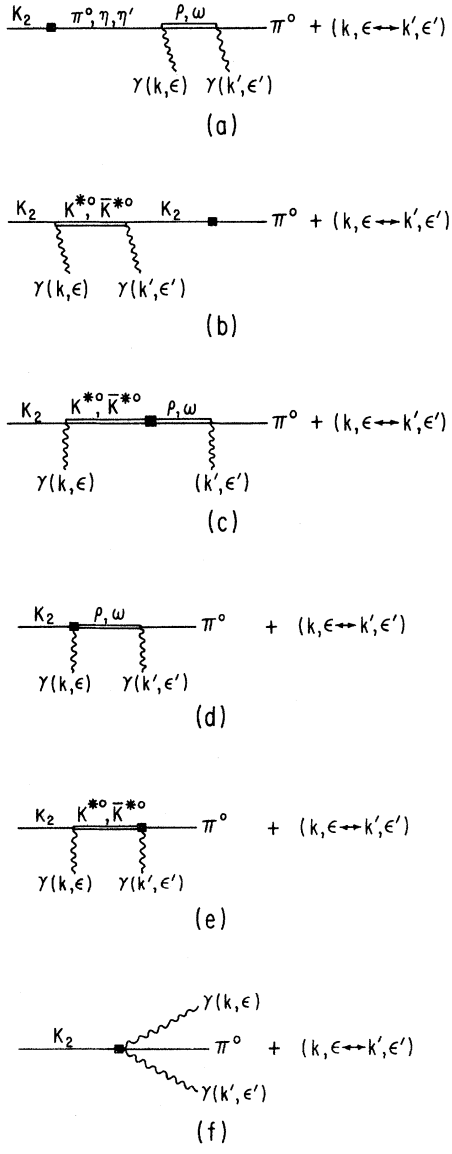

FIG. 13. Feynman diagrams for $K_L \to \pi^0 \gamma\gamma$ of $O(p^6)$: (a)–(e) with vector mesons, (f) without vector mesons (Sec. VI B).

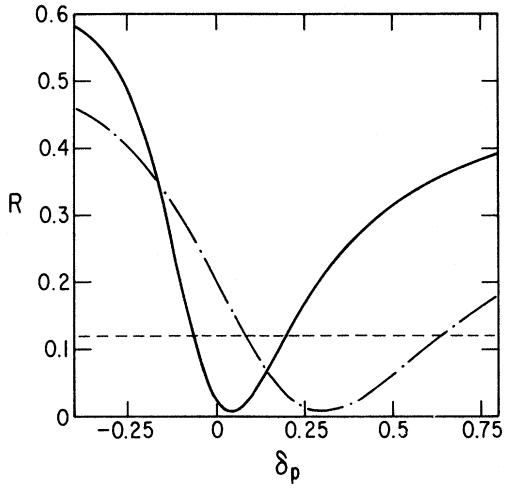

FIG. 14. R vs δ_p: without vector mesons (dash-dotted line, Sec. VI B); with vector mesons with $\delta_n = 0.54$ (solid line). The horizontal line is $R_{\text{expt}} = 0.12$.

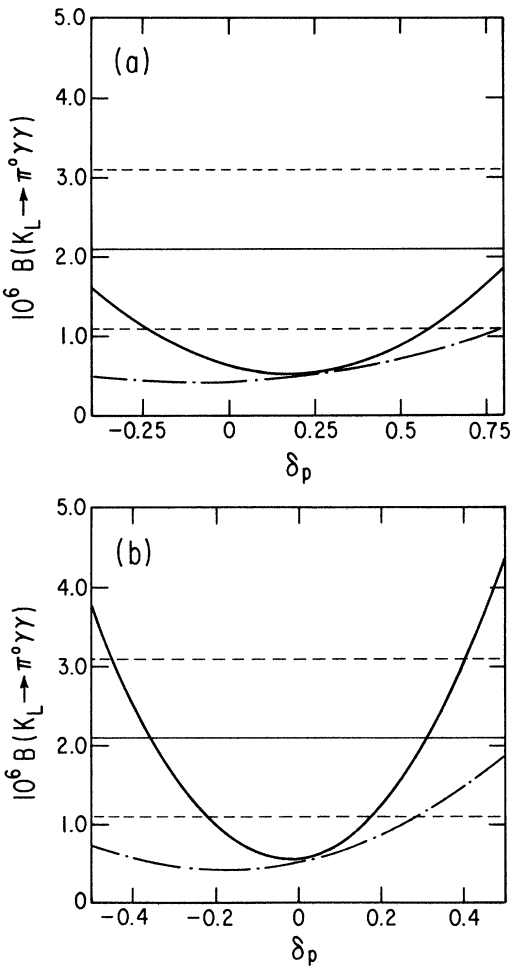

FIG. 15. $B(K_L \to \pi^0\gamma\gamma)$ vs δ_p with (dash-dotted line) and without (solid line) the cut $m_{\gamma\gamma} \geq 280$ MeV: (a) without vector mesons (Sec. VI B), (b) with vector mesons with $\delta_n = 0.54$. Horizontal lines are the data with the cut at 90% C.L.

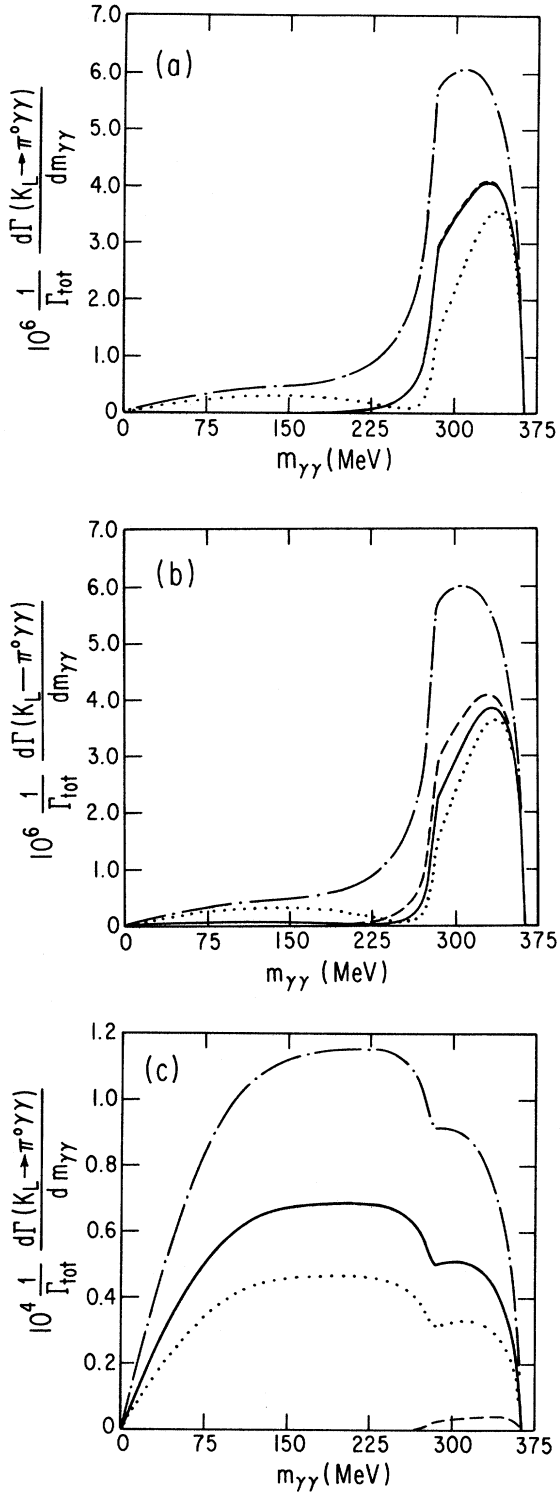

FIG. 16. The spectrum of two photons in $K_L \to \pi^0\gamma\gamma$. (a) Without vector mesons (Sec. VI B): dotted line for $\delta_p = 0.08$, solid line for $\delta_p = 0.33$, and dash-dotted line for $\delta_p = 0.64$. (b) With vector mesons with $\delta_n = 0.54$: dotted line for $\delta_p = -0.06$, solid line for $\delta_p = 0.0$, and dash-dotted line for $\delta_p = 0.20$. (c) With vector mesons with $\delta_n = 0.13$: dotted line for $\delta_p = -1.9$, solid line for $\delta_p = -1.5$, and dash-dotted line for $\delta_p = -1.2$. Dashed line for ChPT to $O(p^4)$ (chiral loop) in (a), (b), and (c).

$$F(z)=\begin{cases}1-\frac{4}{z}[\arcsin(\sqrt{z}/2)]^2 & (z\le 4)\ ,\\ 1+\frac{1}{z}\left[\ln\left(\frac{1+\sqrt{1-4/z}}{1-\sqrt{1-4/z}}\right)-i\pi\right]^2 & (z\ge 4)\ ,\end{cases}$$

and

$$s=(P-p)^2=(k+k')^2=2k\cdot k'\ ,$$

$$t=(P-k)^2=m_{K_L}^2-2P\cdot k\ ,$$

$$u=(P-k')^2=m_{K_L}^2-2P\cdot k'\ .$$

We simply note that this amplitude contains only a $\Delta I=\frac{1}{2}$ contribution.

B. What happens without vector mesons?

If we did not consider vector mesons at all, we would reach the same trouble as we encountered in the study of $W\to\pi\gamma$ and $K_L\to\gamma l^+l^-$. The troublemaker is the same as before: the anomalous current from the Wess-Zumino anomaly has nonvanishing $\pi\gamma$ component:

$$j_L^{\rm WZ}(\pi\gamma)=\frac{30Cie}{f_\pi}\{d\pi,Q\,dA\}\ .$$

This current, by itself, generates the effective weak Lagrangian (we consider the octet piece only for simplicity)

$$-\frac{C_8^{(1/2)}G_F}{\sqrt{2}}\frac{\alpha}{64\pi^3f_\pi^2}\{F_{\alpha\beta}F^{\alpha\beta}[\partial^\nu\pi^+\partial_\nu K^-+\partial^\nu\pi^-\partial_\nu K^+-4(1-3\delta_p)\partial^\nu\pi^0\partial_\nu K_2]$$
$$+2F_{\alpha\beta}F^{\beta\nu}[\partial^\nu\pi^-\partial_\alpha K^++\partial^\nu\pi^+\partial_\alpha K^--4(1-3\delta_p)\partial^\nu\pi^0\partial_\alpha K_2]\}\ . \tag{68}$$

This produces two photons both in $J=0$ and $J=2$ states, and its contributions to $A_{\rm ch}$ and $B_{\rm ch}$ amplitudes are [see Fig. 13(f)]

$$A_{\rm ch}^{\rm WZ}=\frac{C_8^{(1/2)}G_F}{\sqrt{2}}\frac{\alpha}{16\pi^3f_\pi^2}(1-3\delta_p)(3m_K^2+m_\pi^2-s)\ ,$$
$$B_{\rm ch}^{\rm WZ}=\frac{C_8^{(1/2)}G_F}{\sqrt{2}}\frac{\alpha}{16\pi^3f_\pi^2}(1-3\delta_p)2s\ . \tag{69}$$

This is the only $O(p^6)$ contribution in the absence of vector mesons, and corresponds to $a_V=0.7(1-3\delta_p)$ in the notation of Ecker *et al.* [56]. It should be emphasized that existence of this amplitude and its dependence on δ_p have nothing to do with $U(3)_f$ instead of $SU(3)_f$ or vector mesons. They result from the left-handed current $j_L^{\rm WZ}(\pi\gamma)$ and its trace being nonzero. We also note that only $K_L\to\pi^0\gamma\gamma$ is affected by δ_p. For arbitrary values of δ_p, we note that a_V can be either positive or negative. In other words, we can have either destructive or constructive interference between the chiral loop amplitude [Eq. (68)] of $O(p^4)$ and the $O(p^6)$ chiral amplitude [Eq. (70)] originating from $\Gamma_{\rm WZ}$, even in the absence of vector mesons.

From the measurement of the two-photon spectrum $R_{\rm expt}$ we can get information on δ_p. In Fig. 14, we plot R vs δ_p (dash-dotted line), and $R_{\rm expt}<0.12$ at 90% C.L. (dashed line). We find the allowed range for δ_p is

$$0.08\le\delta_p\le 0.64\ .$$

In Fig. 15(a), we show the branching ratio of $K_L\to\pi^0\gamma\gamma$ with and without the cut ($m_{\gamma\gamma}\ge 280$ MeV), and find that

$$4.5\times10^{-7}\le B(K_L\to\pi^0\gamma\gamma)_{\rm cut}\le 8.8\times10^{-7}$$

and

$$5.6\times10^{-7}\le B(K_L\to\pi^0\gamma\gamma)\le 12.7\times10^{-7}\ .$$

Two-photon spectra for $\delta_p=0.08$ (dotted), 0.33 (solid),

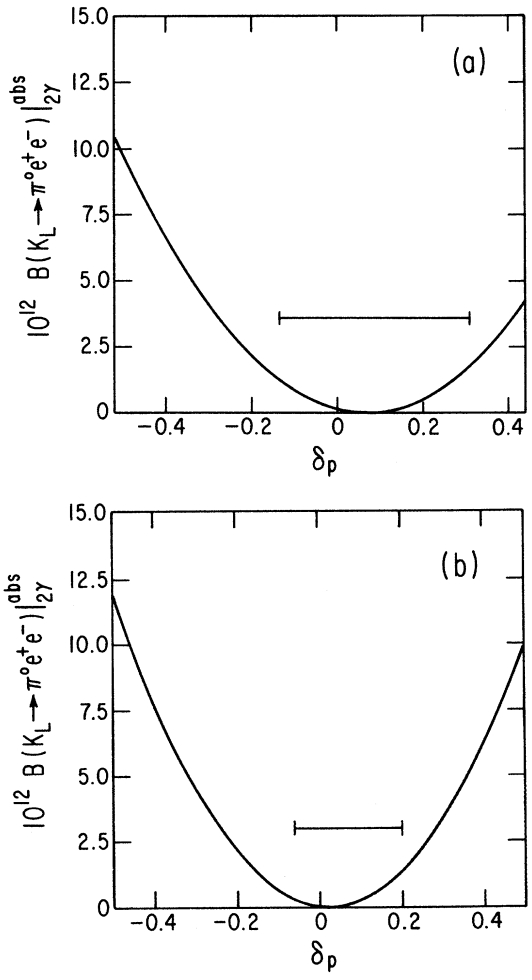

FIG. 17. $B(K_L\to\pi^0e^+e^-)|_{2\gamma}^{\rm abs}$ vs δ_p: (a) without vector mesons (Sec. VI B), (b) with vector mesons with $\delta_n=0.54$. Allowed ranges of δ_p from $R\le 0.12$ are shown in the horizontal bars.

and 0.64 (dash-dotted) are shown in Fig. 16(a) along with $O(p^4)$ CPT prediction (dashed). For δ_p in this range, the imaginary part of the *CP*-conserving two-photon contribution to $K_L \to \pi^0 e^+ e^-$ is constrained to be

$$B(K_L \to \pi^0 e^+ e^-)|^{\rm abs}_{2\gamma} \leq 1.8 \times 10^{-12} ,$$

using the result of Ref. [56]. It is very small for a certain range of δ_p. [See Fig. 17(a).] Lacking the precise measurement of $B(K_L \to \pi^0 \gamma\gamma)$, we cannot get better a constraint on δ_p. This upper bound on $B(K_L \to \pi^0 e^+ e^-)|^{\rm abs}_{2\gamma}$ is marginal and it can interfere with the direct *CP*-violating amplitude if the branching ratio of the latter is of order 10^{-12}. The δ_p obtained in this subsection is less favored than the δ_p obtained in Sec. V C and the next subsection, since (i) we did not include the vector meson contributions to $K_L \to \pi^0\gamma\gamma$ here and (ii) the form factor of e^+e^- is slightly shifted upwards from the best fit in Sec. V C. [See Fig. 11(a) for $\delta_p = 0.64$; the thin solid line for example.] But, reason (ii) is less stringent than (i).

C. Vector-meson contributions to $K_L \to \pi^0\gamma\gamma$

In this subsection, we will concentrate on the A_V and B_V amplitudes which are $O(p^6)$. To produce two photons both in $J=0$ and in $J=2$, we need two vertices with the Levi-Civita tensor, i.e., two vertices from the Wess-Zumino anomaly. The Wess-Zumino anomaly contains $VP\gamma$ vertices, which generate the Feynman diagrams in Fig. 13. Only Fig. 13(a) was considered in the previous analysis [4,5]. Figure 13(b) was neglected because it is suppressed by factor $m_\pi^2/m_{K_L}^2$ compared with Fig. 13(a). This is not true if $\delta_n = 0.54$, for which the η pole dominates in $K_L \to \gamma\gamma$. Therefore, we include this diagram in this paper. All the other diagrams are generated by the left-handed currents containing vector-meson fields. In particular, Figs. 13(d) and 13(e) have weak $V\pi\gamma$ vertices, whose effects were already seen in the previous section on $K_L \to \gamma l^+ l^-$. In passing, we remark that there is no sign ambiguity at all between the $O(p^4)$ chiral loop amplitude and the $O(p^6)$ vector meson amplitudes, since all the amplitudes are generated from the same Lagrangian.

First, we consider Fig. 13(a). From the result of Ref. [5], we have

$$A_V^{(a)} = \sum_{V=\rho^0,\omega} G_V [f_V(t)(t+m_K^2) + f_V(u)(u+m_K^2)] ,$$
$$B_V^{(a)} = \sum_{V=\rho^0,\omega} G_V s [f_V(t) + f_V(u)] . \tag{70}$$

The coupling constants G_V's are of the form

$$G_\rho = -\frac{g^2_{\omega\pi^0\gamma}}{2m_\rho^2} \frac{a(K_2\pi^0)}{m_{K_2}^2} \left[\frac{1}{9} \frac{1}{1-r_\pi^2} + \frac{1}{3} \frac{\xi}{1-r_\eta^2} X_{\eta\rho} + \frac{1}{3} \frac{\xi'}{1-r_{\eta'}^2} X_{\eta'\rho} \right] ,$$

$$G_\omega = -\frac{g^2_{\omega\pi^0\gamma}}{2m_\omega^2} \frac{a(K_2\pi^0)}{m_{K_2}^2} \left[\frac{1}{1-r_\pi^2} + \frac{1}{3} \frac{\xi}{1-r_\eta^2} X_{\eta\rho} + \frac{1}{3} \frac{\xi'}{1-r_{\eta'}^2} X_{\eta'\rho} \right] ,$$

where $X_{\eta\rho}$ and $X_{\eta'\rho}$ are defined in Eq. (53). First of all, from Eqs. (3) and (16) we can show that

$$g^2_{\omega\pi^0\gamma} = \frac{9\alpha}{32\pi^3 f_\pi^2} \frac{m_V^2}{f_\pi^2} .$$

Next, using the values of δ_n obtained in Sec. V, we find that $G_V m_{K_L}^2 (\equiv G_\rho m_{K_L}^2 + G_\omega m_{K_L}^2)$ has two possible values:

$$G_V m_{K_L}^2 = \frac{G_F m_K^4}{\sqrt{2}} \frac{\alpha}{16\pi^3 f_\pi^2} \wp \frac{9}{2} \left[\frac{10}{9} \frac{1}{1-r_\pi^2} + \frac{2}{3} \left[\frac{\xi}{1-r_\eta^2} X_{\eta\rho} + \frac{\xi'}{1-r_{\eta'}^2} X_{\eta'\rho} \right] \right]$$
$$= \begin{cases} 3.3 \times 10^{-9} & \text{for } \delta_n = 0.13 , \\ 0.2 \times 10^{-9} & \text{for } \delta_n = 0.54 . \end{cases} \tag{71}$$

The first one is essentially the same as one taken in the previous analysis [4,5] assuming naive nonet symmetry for $a(K_2\pi^0)$, $a(K_2\eta_8)$, and $a(K_2\eta_0)$. However, we will see that the second one is preferred by the form factor in $K_L \to \gamma l^+ l^-$ and the two-photon spectrum in $K_L \to \pi^0\gamma\gamma$, if we include the vector meson contributions in a systematic way.

Figure 13(b) can be evaluated in the same way as Fig. 13(a), and the result is

$$A_V^{(b)} = G_{K^*}[(t+m_K^2) f_{K^*}(t) + (u+m_K^2) f_{K^*}(u)] ,$$
$$B_V^{(b)} = G_{K^*}[f_{K^*}(t) + f_{K^*}(u)] , \tag{72}$$

where

$$G_{K^*} m_K^2 = -\frac{G_F m_K^4}{\sqrt{2}} \frac{\alpha}{16\pi^3 f_\pi^2} \frac{2\wp r_\pi^2}{1-r_\pi^2} . \tag{73}$$

This is negligible compared to Eq. (71) with $\delta_n = 0.13$, but it is not true for Eq. (71) with $\delta_n = 0.54$.

In our model, we have three more diagrams which were not considered in the previous studies [see Figs. 13(c)–13(e)]. In these diagrams, the vector-meson exchange is essential. Figure 13(c) contains one normal weak vertex and two anomalous $VP\gamma$ vertices. This diagram gives

$$A_V^{(c)}=\frac{G_F}{\sqrt{2}}\frac{\alpha}{16\pi^3 f_\pi^2}[C_8^{(1/2)}(1-3\delta_p)+4C_{27}^{(1/2)}+C_{27}^{(3/2)}]$$
$$\times[f_{K^*}(t)f_\rho(t)(m_K^2+t)+f_{K^*}(u)f_\rho(u)(m_K^2+u)]\ ,$$
$$B_V^{(c)}=\frac{G_F}{\sqrt{2}}\frac{\alpha}{16\pi^3 f_\pi^2}[C_8^{(1/2)}(1-3\delta_p)+4C_{27}^{(1/2)}+C_{27}^{(3/2)}]$$
$$\times s[f_{K^*}(t)f_\rho(t)+f_{K^*}(u)f_\rho(u)]\ . \tag{74}$$

Figures 13(d) and 13(e) are generated by anomalous weak $V\pi\gamma$ vertices. The relevant effective weak Lagrangians were given in Eqs. (56)–(58) when we discussed $K_L\to\gamma l^+l^-$. The ρ and ω exchange diagrams [Fig. 13(d)] yield

$$A_V^{(d)}=-\frac{G_F}{\sqrt{2}}\frac{\alpha}{16\pi^3 f_\pi^2}[\,C_8^{(1/2)}(1+3\delta_p)$$
$$-2C_{27}^{(1/2)}+5C_{27}^{(3/2)}]$$
$$\times\tfrac{1}{2}[f_\rho(t)(m_K^2+t)+f_\rho(u)(m_K^2+u)]\ ,$$
$$B_V^{(d)}=-\frac{G_F}{\sqrt{2}}\frac{\alpha}{16\pi^3 f_\pi^2}[C_8^{(1/2)}(1+3\delta_p)-2C_{27}^{(1/2)}+5C_{27}^{(3/2)}]$$
$$\times\frac{s}{2}[f_\rho(t)+f_\rho(u)]\ . \tag{75}$$

The K^* exchange generates Fig. 13(e) with

$$A_V^{(e)}=-\frac{G_F}{\sqrt{2}}\frac{\alpha}{16\pi^3 f_\pi^2}[C_8^{(1/2)}+C_{27}^{(1/2)}-2C_{27}^{(3/2)}]$$
$$\times\tfrac{1}{2}[f_{K^*}(t)(m_K^2+t)+f_{K^*}(u)(m_K^2+u)]\ ,$$
$$B_V^{(e)}=-\frac{G_F}{\sqrt{2}}\frac{\alpha}{16\pi^3 f_\pi^2}[C_8^{(1/2)}+C_{27}^{(1/2)}-2C_{27}^{(3/2)}]$$
$$\times\frac{s}{2}[f_{K^*}(t)+f_{K^*}(u)]\ . \tag{76}$$

We can observe that there are large cancellations among diagrams with weak VV vertices and diagrams with weak $V\pi\gamma$ vertices both in $K_L\to\gamma l^+l^-$ and $K_L\to\pi^0\gamma\gamma$ as long as $\delta_p=0$. We expect this to be a general phenomenon.

First, let us consider R in case all the vector meson contributions are taken into account. From Fig. 14 (solid line), we find that

$$-0.06\le\delta_p\le 0.20 \quad \text{for } \delta_n=0.54\ . \tag{77}$$

For this range of δ_p, the branching ratio of $B(K_L\to\pi^0\gamma\gamma)$ with and without the cut is [see Fig. 15(b)]

$$4.6\times10^{-7}\le B(K_L\to\pi^0\gamma\gamma,\ m_{\gamma\gamma}\ge 280\ \text{MeV})$$
$$\le 8.7\times10^{-7}\ , \tag{78}$$
$$5.8\times10^{-7}\le B(K_L\to\pi^0\gamma\gamma)\le 12.6\times10^{-7}\ . \tag{79}$$

In particular, $B(K_L\to\pi^0\gamma\gamma)=5.7\times10^{-7}$ for $\delta_p=0$. This is slightly smaller than the predictions by CPT and the pion rescattering model, $(6.3 \text{ and } 7.5)\times10^{-7}$, respectively. In Table III, we give R, $B(K_L\to\pi^0\gamma\gamma)_{\rm cut}$, $B(K_L\to\pi^0\gamma\gamma)$ for different values of δ_p in the case $\delta_n=0.54$. Considering the intrinsic uncertainties in the calculations based on the effective Lagrangian or current algebra and PCAC, the isospin breaking effect which is neglected, and the experimental error, it would be difficult to distinguish various predictions. We note that this range of δ_p is compatible with that obtained in Sec. V C and is actually more stringent.

One of the main messages of this paper is that there is a small range of δ_p or $\delta_n=0.54$, for which (i) the prediction of the form factor of e^+e^- in $K_L\to\gamma e^+e^-$ agrees with the recent measurement, and (ii) the two-photon spectrum at low $m_{\gamma\gamma}$ is not as enhanced as reported in the previous analyses but consistent with the measurement if we correctly include the vector-meson contribu-

TABLE III. R, $B(K_L\to\pi^0\gamma\gamma)_{\rm cut}$, $B(K_L\to\pi^0\gamma\gamma)$, and $B(K_L\to\pi^0e^+e^-)_{2\gamma}^{\rm abs}$ for different values of δ_p for $\delta_n=0.54$.

δ_p	R (%)	$B(K_L\to\pi^0\gamma\gamma)_{\rm cut}$ (10^{-7})	$B(K_L\to\pi^0\gamma\gamma)$ (10^{-7})	$B(K_L\to\pi^0e^+e^-)_{2\gamma}^{\rm abs}$ (10^{-12})
−0.06	11.4	4.6	5.8	0.30
−0.04	7.7	4.8	5.7	0.17
−0.02	4.7	5.0	5.6	0.08
0.00	2.5	5.2	5.7	0.02
0.02	1.2	5.5	5.9	2×10^{-4}
0.04	0.7	5.7	6.2	0.01
0.06	1.0	6.0	6.6	0.06
0.08	1.8	6.3	7.1	0.15
0.10	3.1	6.7	7.8	0.26
0.12	4.7	7.0	8.5	0.41
0.14	6.5	7.4	9.3	0.61
0.16	8.4	7.8	10.3	0.83
0.18	10.3	8.3	11.4	1.09
0.20	12.3	8.7	12.6	1.38

tions. If we choose $\delta_n=0.13$ and $-1.9\le\delta_p\le-1.2$ obtained in Sec. V C, we get too large values of R and $B(K_L\to\pi^0\gamma\gamma)$ that are not consistent with the experimental data. We show two-photon spectra for certain values of δ_p in Fig. 16(b) for $\delta_n=0.54$ and in Fig. 16(c) for $\delta_n=0.13$. Figure 16(c) is clearly excluded by too large $R_{\rm expt}$ and branching ratio:

$$2.6\times10^{-5}\le B(K_L\to\pi^0\gamma\gamma)\le6.4\times10^{-5}$$
$$\text{for } -1.9\le\delta_p\le-1.2 .$$

We note that our predictions for $B(K_L\to\pi^0\gamma\gamma)$ are less than the data by more than one standard deviation. As far as our model is concerned, however, there is no way to make the branching ratio consistent with the data. Any attempts lead to inconsistency with other data. We would have to await more refined measurement of $K_L\to\pi^0\gamma\gamma$ to say more about comparison of the theory and the experimental data. If we include vector mesons in the hidden-symmetry scheme, the only solution which leads to a consistent description of the available data on rare kaon decays (except $K_L\to\pi^+\pi^-\gamma$) is

$$\delta_n=0.54,\quad -0.06\le\delta_p\le0.20 . \tag{80}$$

Considering $\delta_p-\delta_n$ measures nonet symmetry breaking in our approach, Eq. (80) corresponds to the case with nonet symmetry not badly broken. [See also Eq. (62).] For $\delta_n=0.54$, we have $\zeta=0.54$ and $\zeta'=-0.57$. If nonet symmetry were not broken at all, we would have $\zeta=0.02$ and $\zeta'=-1.94$. Other choices are not compatible either with the measurement of the form factor of $K_L\to\gamma e^+e^-$ or with the observed two-photon spectrum in $K_L\to\pi^0\gamma\gamma$.

D. Implications for $K_L\to\pi^0e^+e^-$

To study the two-photon contribution to $K_L\to\pi^0e^+e^-$, we first consider the limit of infinitely heavy vector mesons. In this limit, we have $f_V=1$, equivalent to setting $t=u=0$ in the arguments of f_V. Then, the invariant amplitude A_V becomes

$$A_V(s,0,0)=\frac{G_F}{\sqrt{2}}\frac{\alpha}{16\pi^3f_\pi^2}C_8^{(1/2)}\tilde{a}_V(3m_K^2+m_\pi^2-s) , \tag{81}$$

and a similar expression for $B_V(s,0,0)$. Our $\tilde{a}_V$ is related to a_V in Ref. [55] by

$$a_V=0.7\tilde{a}_V .$$

We list each contribution to $\tilde{a}_V$ from Figs. 13(a)–13(e) in Table IV. There is a cancellation of the octet amplitudes among Figs. 13(c)–13(e) in this limit. In total, we have

$$\tilde{a}_V=(0.10-4.50\delta_p)\quad\text{for } \delta_n=0.54 ,$$

so that

$$-0.80\le\tilde{a}_V\le+0.37 ,$$

or

$$-0.56\le a_V\le0.26 . \tag{82}$$

This value of a_V is consistent with zero.

TABLE IV. Contributions to $C_8^{(1/2)}\tilde{a}_V$ of each diagram in Fig. 13. $\tilde{a}_V$ is defined in Eq. (82).

Fig. 13(i)	$C_8^{(1/2)}\tilde{a}_V^{(i)}$
(a)	$\frac{9}{2}\wp\left[\frac{10}{9}\frac{1}{1-r_\pi^2}+\frac{2}{3}\left[\frac{\zeta}{1-r_\eta^2}X_{\eta\rho}+\frac{\zeta'}{1-r_{\eta'}^2}X_{\eta'\rho}\right]\right]$
(b)	$\frac{2\wp r_\pi^2}{1-r_\pi^2}$
(c)	$C_8^{(1/2)}(1-\delta_p)+4C_{27}^{(1/2)}+C_{27}^{(3/2)}$
(d)	$-\frac{1}{2}[C_8^{(1/2)}(1+\delta_p)-2C_{27}^{(1/2)}+5C_{27}^{(3/2)}]$
(e)	$-\frac{1}{2}(C_8^{(1/2)}+C_{27}^{(1/2)}-2C_{27}^{(3/2)})$
Total	$C_8^{(1/2)}(0.10-4.50\delta_p)$

Our result on $K_L\to\pi^0\gamma\gamma$ implies that the *CP*-conserving two-photon contribution to $K_L\to\pi^0e^+e^-$ is less than 1.4×10^{-12} in the branching ratio [Fig. 17(b)], using the result of Ecker *et al.* [56]. The direct *CP*-violating contribution to $K_L\to\pi^0e^+e^-$ is estimated to be around 10^{-11} [12]. In viewing the result of Sec. IV on $K_S\to\pi^0e^+e^-$, we expect that $K_L\to\pi^0e^+e^-$ occurs mainly through the indirect *CP*-violating one-photon-exchange process with $B(K_L\to\pi^0e^+e^-)\simeq(1.4$ or $2.7)\times10^{-10}$. The present upper limit is still far above our model (about a factor of 20 or so). However, there is a chance that this level of sensitivity can be reached by experiments in the near future. Since ChPT predicts a smaller branching ratio for this decay mode, observation of the signal at the level of 10^{-10} should be able to distinguish between these two predictions, and will provide us with an important piece of information regarding the effects of long-distance physics in nonleptonic kaon decays.

VII. SUMMARY AND OUTLOOK

A. Summary of the results

In the present paper, we studied a certain class of kaon decays where the effects of vector mesons are important. From our Lagrangian, Eq. (1), the left-handed current could be constructed in a unique way. Vector-meson contributions to the left-handed current generated some weak vertices containing vector mesons, such as *weak* $V\pi\pi$, VV, $V\pi\gamma$, etc. In particular, we included the anomalous left-handed current constructed from the Wess-Zumino anomaly $\Gamma_{\rm WZ}$ and $\Gamma_V^{\rm anom}$. These new vertices were important to understand $K_L\to\gamma l^+l^-$ and $K_L\to\pi^0\gamma\gamma$ in a systematic way. These new vertices generate new Feynman diagrams and give the predictions for $K_L\to\gamma e^+e^-$ and $K_L\to\pi^0\gamma\gamma$ which are consistent with the data for a certain choice of parameters.

In $K^+\to\pi^+e^+e^-$, we could determine $C_7=-0.01^{+0.03}_{-0.04}$ or $-0.61^{+0.03}_{-0.04}$ from the best fit to $B(K^+\to\pi^+e^+e^-)$. This parameter measures the short-distance contribution of the electromagnetic penguin diagram to the process $K\to\pi l^+l^-$. The twofold ambiguity

can be lifted by the spectrum measurement of $K^+ \to \pi^+ e^+ e^-$ at low m_{ee}. For either value of C_7, we are led to rather large branching ratios for the indirect CP-violating $K_L \to \pi^0 e^+ e^-$ at the level of a few parts in 10^{-10}. We found that the form factor $|F_{K_2\gamma\gamma}(s)|^2$ measured in $K_L \to \gamma e^+ e^-$ has some correlation with the two-photon spectrum for $K_L \to \pi^0 \gamma\gamma$. This correlation comes through ζ and ζ' or δ_n defined in Sec. V. Introducing a parameter δ_n characterizing nonet-symmetry breaking in $a(K_2\eta_0)/a(K_2\pi^0)$, we find that $\delta_n = 0.54$ gives correct spectra both for the form factor in $K_L \to \gamma e^+ e^-$ and $K_L \to \pi^0\gamma\gamma$ for $-0.06 \le \delta_p \le 0.20$.

Summarizing, the choice of $\delta_n = 0.54$ and $-0.06 \le \delta_p \le 0.20$ gives satisfactory descriptions for $K_L \to \gamma\gamma$, $K_L \to \gamma e^+ e^-$, and $K_L \to \pi^0\gamma\gamma$. It is important to include the anomalous left-handed current to describe $K_L \to \gamma l^+ l^-$ and $K_L \to \pi^0\gamma\gamma$. We predict $B(K_L \to \gamma\mu^+\mu^-) \simeq 4.3 \times 10^{-7}$, and this is one of the tests that can distinguish our model from others. We also predict that the branching ratio of $K_L \to \pi^0 e^+ e^-$ is about $(1.4 \text{ or } 2.7) \times 10^{-10}$, and it is mainly indirectly CP violating. This is larger than the lowest order ChPT prediction, and it should be a crucial test of our model.

B. Outlook

We can try to improve our calculations within our model. In Sec. II B, we considered symmetry-breaking effects, and calculated electromagnetic charge radii of π^+, K^+, and K^0. (See Table I.) And then we chose $c_A = c_V = 0$ for simplicity. We note that $c_A = 0.49$ and $c_V = 0$ give the right relations for vector-meson masses and electromagnetic charge radii of π^+, K^+, and K^0. Therefore, we may choose this set of parameters. Then, the left-handed current contains a small piece with a $\pi\pi$ component, and the weak Lagrangian has new $\pi\pi\pi$ and $V\pi\pi$ vertices, and complete vector-meson dominance is broken even for $a = 2$. Another improvement can be made for the choice of a. We chose $a = 2$ in this paper. However, $a = 2.16$ gives a better fit to $m_\rho^2 = a g^2 f_\pi^2$ and $\Gamma(\rho \to \pi\pi)$. For this value of a, complete vector-meson dominance is slightly broken, and we get a better number for the electromagnetic charge radius of π^+. This kind of improvement may affect the analysis of $K_S \to \pi^0 e^+ e^-$ a lot, since we already noticed it in the electromagnetic charge radius of K^0. Also, the resonance nature of vector mesons, which was neglected in this paper, should be implemented if possible.

To improve our understanding of kaon decays, we need the effective Lagrangian which is successful in the phenomenology of strong and electromagnetic interactions of pseudoscalar mesons and vector mesons (and axial-vector mesons, if possible). In particular, $SU(3)_f$-symmetry-breaking effects should be encoded in the effective Lagrangian in such a way that the theoretical predictions agree with the low-energy data, e.g., electromagnetic charge radii of mesons, $\pi\pi$ scattering length, $\gamma\gamma \to \pi\pi$, and many more. We also need more precise measurements of these quantities to establish the validity of such an effective Lagrangian. Furthermore, we need to know how the Wilson coefficients and the hadronic matrix elements depend on the scale below ~ 1 GeV. Then we can probe the structure of the weak Hamiltonian, and after all, we may be able to find the relations between the quark picture and the meson picture which can explain the nonleptonic kaon decays including the $\Delta I = \frac{1}{2}$ rule [36].

ACKNOWLEDGMENTS

It is my pleasure to express deep gratitude to Professor J. L. Rosner for continuing discussions, suggestions, and encouragements during my Ph.D. course and carefully reading the manuscript. He also thanks Professor T. N. Truong for useful discussions especially on $K^+ \to \pi^+ e^+ e^-$ and $K_L \to \pi^0\gamma\gamma$, and for encouragements. Thanks also go to Professor Y. Nambu, Professor B. Winstein, Professor T. Wah, Mr. R. Briere, Dr. V. Papadimitriou, and Dr. H. Yamamoto for discussions and comments on various points, especially on experimental status. This work was supported by United States Department of Energy under Grant No. DE-FG02-90ER-40560, presented as a thesis to the Department of Physics, The University of Chicago, in partial fulfillment of the requirements for the Ph.D. degree.

[1] G. Ecker, A. Pich, and E. de Rafael, Phys. Lett. B **189**, 363 (1987); Nucl. Phys. **B303**, 665 (1988).
[2] L. M. Sehgal, Phys. Rev. D **38**, 808 (1988); T. Morozumi and H. Iwasaki, KEK Report No. TH-206, 1988 (unpublished); J. Flynn and L. Randall, Reports Nos. UCB-PTH-88-21, LBL-26008, and RAL-88-080 (unpublished).
[3] P. Ko and J. L. Rosner, Phys. Rev. D **40**, 3775 (1989).
[4] L. M. Sehgal, Phys. Rev. D **41**, 161 (1990).
[5] P. Ko, Phys. Rev. D **41**, 1531 (1990).
[6] G. D. Barr *et al.*, Phys. Lett. B **242**, 523 (1990); also, V. Papadimitriou *et al.*, Phys. Rev. Lett. **63**, 28 (1989); V. Papadimitriou, thesis, University of Chicago, 1990.
[7] M. Bando, T. Kugo, and K. Yamawaki, Phys. Rep. **164**, 217 (1988), and references therein.
[8] J. J. Sakurai, Phys. Rev. **156**, 1508 (1967); J. A. Cronin, *ibid.* **161**, 1483 (1967); M. Moshe and P. Singer, Phys. Rev. D **6**, 1379 (1972).
[9] A. I. Vainshtein, V. I. Zakharov, and M. A. Shifman, Zh. Eksp. Teor. Fiz. **72**, 1275 (1977) [Sov. Phys. JETP **45**, 670 (1977)].
[10] F. Gilman and M. Wise, Phys. Rev. D **20**, 2392 (1979).
[11] F. J. Gilman and M. B. Wise, Phys. Rev. D **21**, 3150 (1980).
[12] C. O. Dib, I. Dunietz and F. J. Gilman, Phys. Rev. D **39**, 2639 (1989); J. Flynn and L. Randall, Nucl. Phys. **B326**, 31 (1989); C. O. Dib, thesis, Stanford University, Report No. SLAC-PUB-364, 1990.
[13] G. D. Barr *et al.*, Phys. Lett. B **240**, 283 (1990).
[14] K. E. Ohl *et al.*, Phys. Rev. Lett. **65**, 1407 (1990).
[15] E. Cremmer and B. Julia, Phys. Lett. **80B**, 48 (1978); Nucl.

Phys. **B159**, 141 (1979).
[16] For a nice introduction to this subject, see H. Georgi, *Weak Interactions and Modern Particle Theory* (Benjamin/Cummings, New York, 1984); see also Ref. [7].
[17] K. Kawarabayashi and M. Suzuki, Phys. Rev. Lett. **16**, 255 (1966); Riazuddin and Fayyazuddin, Phys. Rev. **147**, 1071 (1966).
[18] J. J. Sakurai, *Currents and Mesons* (University of Chicago Press, Chicago, 1969).
[19] U.-G. Meissner, Phys. Rep. **161**, 213 (1988).
[20] E. B. Dally *et al.*, Phys. Rev. Lett. **45**, 232 (1980).
[21] W. R. Molzon *et al.*, Phys. Rev. Lett. **41**, 1213 (1978).
[22] L. S. Brown and R. L. Goble, Phys. Rev. Lett. **20**, 346 (1968); Phys. Rev. D **4**, 723 (1971); R. L. Goble, *ibid.* **7**, 931 (1973); T. N. Truong, Ettore Majorana Lectures, Reports Nos. EFI-90-26, A965-0490, and UCSBTH-90-29 (unpublished).
[23] The intrinsic parity (P_0) of a particle is defined to be $+1$, if its parity quantum number P is equal to $(-1)^S$, where S is the spin of the particle. Otherwise, it is -1. Therefore, $P_0(\pi)=-1$, $P_0(\omega)=P_0(\rho)=P_0(\gamma)=+1$, etc.
[24] E. Witten, Nucl. Phys. **B223**, 422 (1983).
[25] J. Wess and B. B. Zumino, Phys. Lett. **37B**, 95 (1971).
[26] S. L. Adler, Phys. Rev. **177**, 2426 (1969); J. S. Bell and R. Jackiw, Nuovo Cimento **60**, 47 (1969).
[27] O. Kaymakcalan, S. Rajeev, and J. Schechter, Phys. Rev. **30**, 594 (1984). We follow their notation using differential forms, when we discuss the anomaly and the anomalous currents. For example, $ABCD \equiv \epsilon_{\mu\nu\alpha\beta} A^\mu B^\nu C^\alpha D^\beta$, and $j^{\text{anom}} = ABC$ means $j^{\text{anom}}_\beta = \epsilon_{\mu\nu\alpha\beta} A^\mu B^\nu C^\alpha$. See also Refs. [24] and [30].
[28] D. J. Gross and R. Jackiw, Phys. Rev. D **6**, 477 (1972).
[29] T. Fujiwara, T. Kugo, H. Terao, S. Uehara, and K. Yamawaki, Prog. Theor. Phys. **73**, 926 (1985).
[30] See, for example, *Lectures on Current Algebra and Its Applications,* edited by Sam B. Treiman, R. Jackiw, and D. J. Gross (Princeton University Press, Princeton, NJ, 1972).
[31] W. A. Bardeen, Phys. Rev. **184**, 1848 (1969).
[32] M. Jacob and T. T. Wu, Phys. Lett. B **232**, 529 (1989).
[33] C. Albajar *et al.*, Phys. Lett. B **241**, 283 (1990).
[34] L. Arnellas, W. Marciano, and Z. Parsa, Nucl. Phys. **B196**, 378 (1982).
[35] A. Pich, B. Guberina, and E. de Rafael, Nucl. Phys. **B277**, 197 (1986).
[36] W. A. Bardeen, A. J. Buras, and J.-M. Gerard, Phys. Lett. B **180**, 133 (1986); **192**, 138 (1987); Nucl. Phys. **B293**, 787 (1987).
[37] T. N. Pham, Phys. Lett. **145B**, 113 (1984).
[38] Particle Data Group, J. J. Hernández *et al.*, Phys. Lett. B **239**, 1 (1990).
[39] K. Kleinknecht, Annu. Rev. Nucl. Sci. **26**, 1 (1976).
[40] M. K. Gaillard and B. W. Lee, Phys. Rev. D **10**, 897 (1974).
[41] P. Bloch *et al.*, Phys. Lett. **56B**, 201 (1975).
[42] G. Ecker, A. Pich, and E. de Rafael, Nucl. Phys. **B303**, 665 (1988).
[43] K. E. Ohl *et al.*, Phys. Rev. Lett. **64**, 2755 (1990).
[44] A. Barker *et al.*, Phys. Rev. D **41**, 3546 (1990).
[45] J. Ellis and J. Hagelin, Nucl. Phys. **B217**, 189 (1983); C. O. Dib, I. Dunietz, and F. J. Gilman, Report No. SLAC-PUB-4840, 1989 (unpublished).
[46] F. J. Gilman and M. Wise, Phys. Rev. D **19**, 976 (1979).
[47] M. K. Gaillard, X. Q. Li, and S. Rudaz, Phys. Lett. **158B**, 158 (1985).
[48] Crystal Ball Collaboration, H. Marsiske *et al.*, in *Proceedings of the VIII International Workshop on Photon-Photon Collisions,* Shoresh, Jerusalem Hills, Israel, 1988, edited by U. Karshon (World Scientific, Singapore, 1988), p. 15.
[49] P. Ko and T. N. Truong, Phys. Rev. D **42**, 2419 (1990).
[50] T. N. Truong, Phys. Lett. B **207**, 495 (1988).
[51] G. D'Ambriosio and D. Espiru, Phys. Lett. B **175**, 237 (1986); J. L. Goity, Z. Phys. C **34**, 341 (1987).
[52] R. L. Goble and J. L. Rosner, Phys. Rev. D **5**, 2354 (1972); R. L. Goble, *ibid.* **7**, 931 (1973); R. L. Goble, R. Rosenfeld, and J. L. Rosner, *ibid.* **39**, 3264 (1989).
[53] H. Burkhardt *et al.*, Phys. Lett. B **199**, 139 (1987).
[54] L. M. Sehgal, Phys. Rev. D **7**, 3303 (1973).
[55] L. Bergström, E. Massó, and P. Singer, Phys. Lett. **131B**, 229 (1983).
[56] G. Ecker, A. Pich, and E. de Rafael, Phys. Lett. B **237**, 481 (1990).